Wavelets, Ridgelets and Curvelets on the Sphere

By: Jean-Luc Starck
Dapnia/SEDI-SAP, Service d'Astrophysique,
CEA-Saclay, France.

Collaborators: Pierick Abrial, Yassir Moudden,Jalal Fadili , Ofer Levi
Emmnauel Candes, David Donoho

1) Motivation for a Curvelet Transform on the Sphere

- The Cosmic Microwave Data Story

  ===> Data restoration

  ===> Detection of cosmological non Gaussian signature

2) The Curvelet Transform

- Comparison of several Curvelet implementations for denoising

3) Wavelet, Ridgelet and Curvelet Transforms on the Sphere

The Big Bang

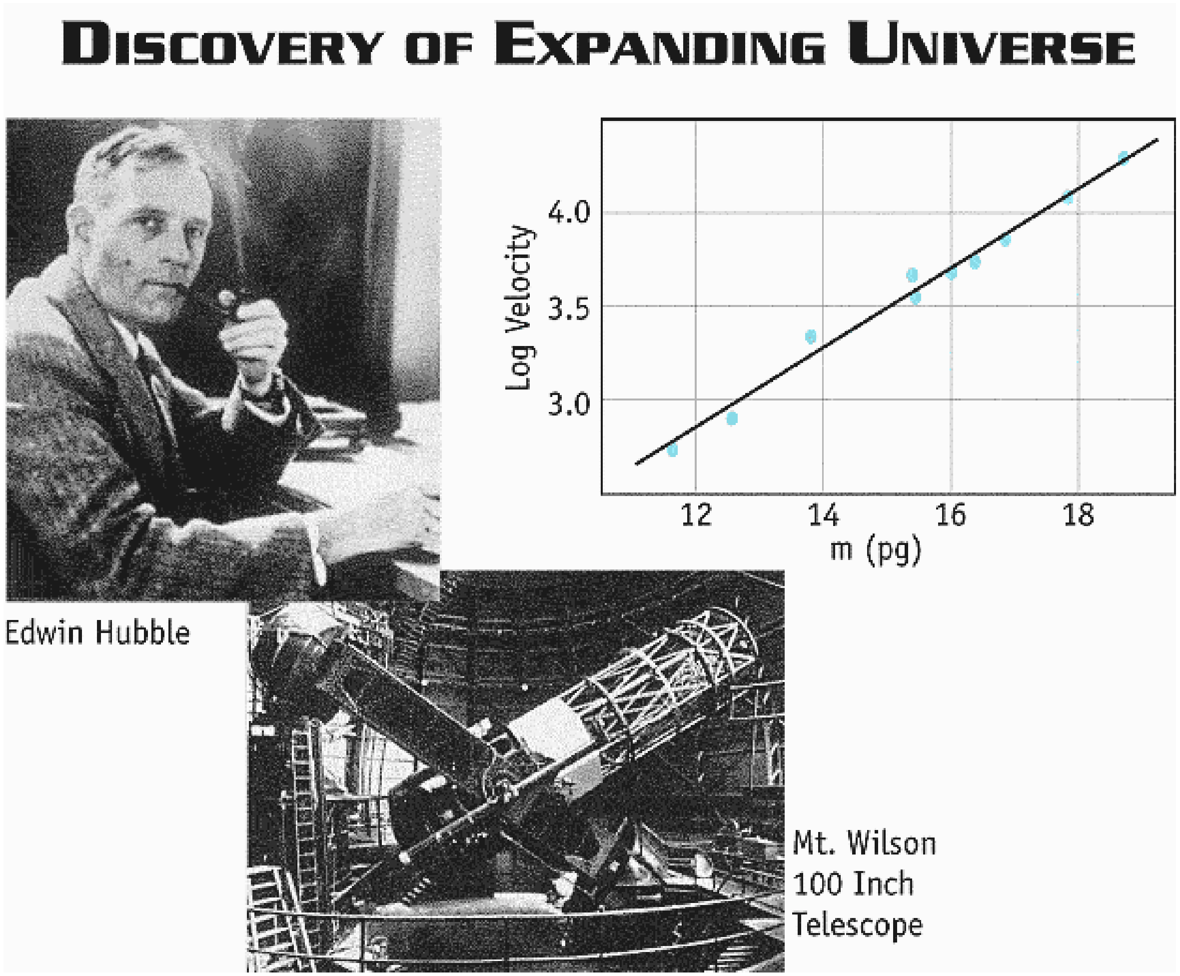
DISCOVERY OF EXPANDING UNIVERSE
Log Velocity
4.0
3.5
3.0
12
14
16
18
m (pg)
Edwin Hubble
Mt. Wilson
100 Inch
Telescope

The Cosmic Microwave Background

- The Universe is filled with a blackbody radiation field at a temperature of 3K.
- Predicted by G. Gamow in 1948
- Observed for the first time by Penzias and Wilson (1965)
- Confirmed by COBE (1990)

The Cosmic Microwave Background

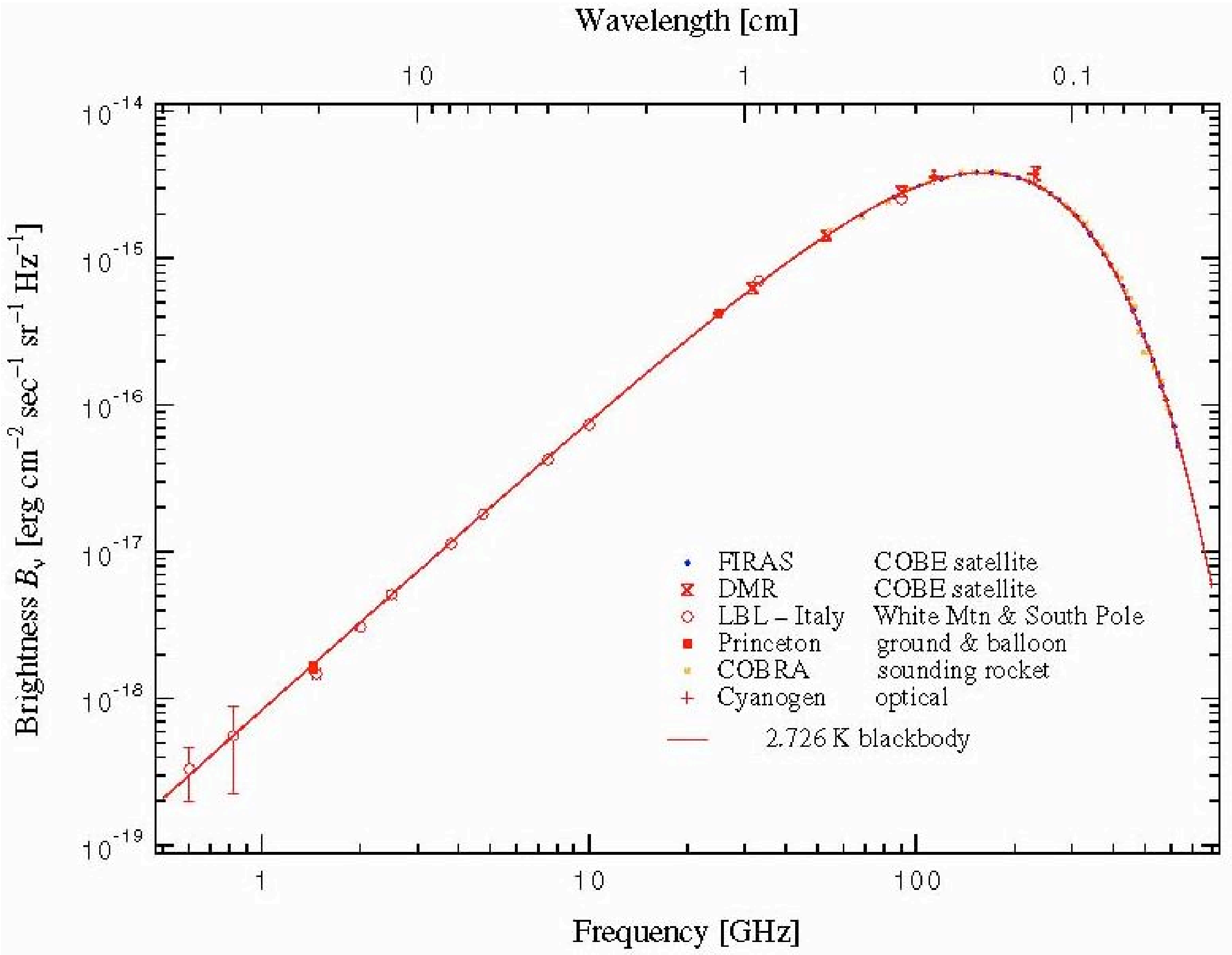

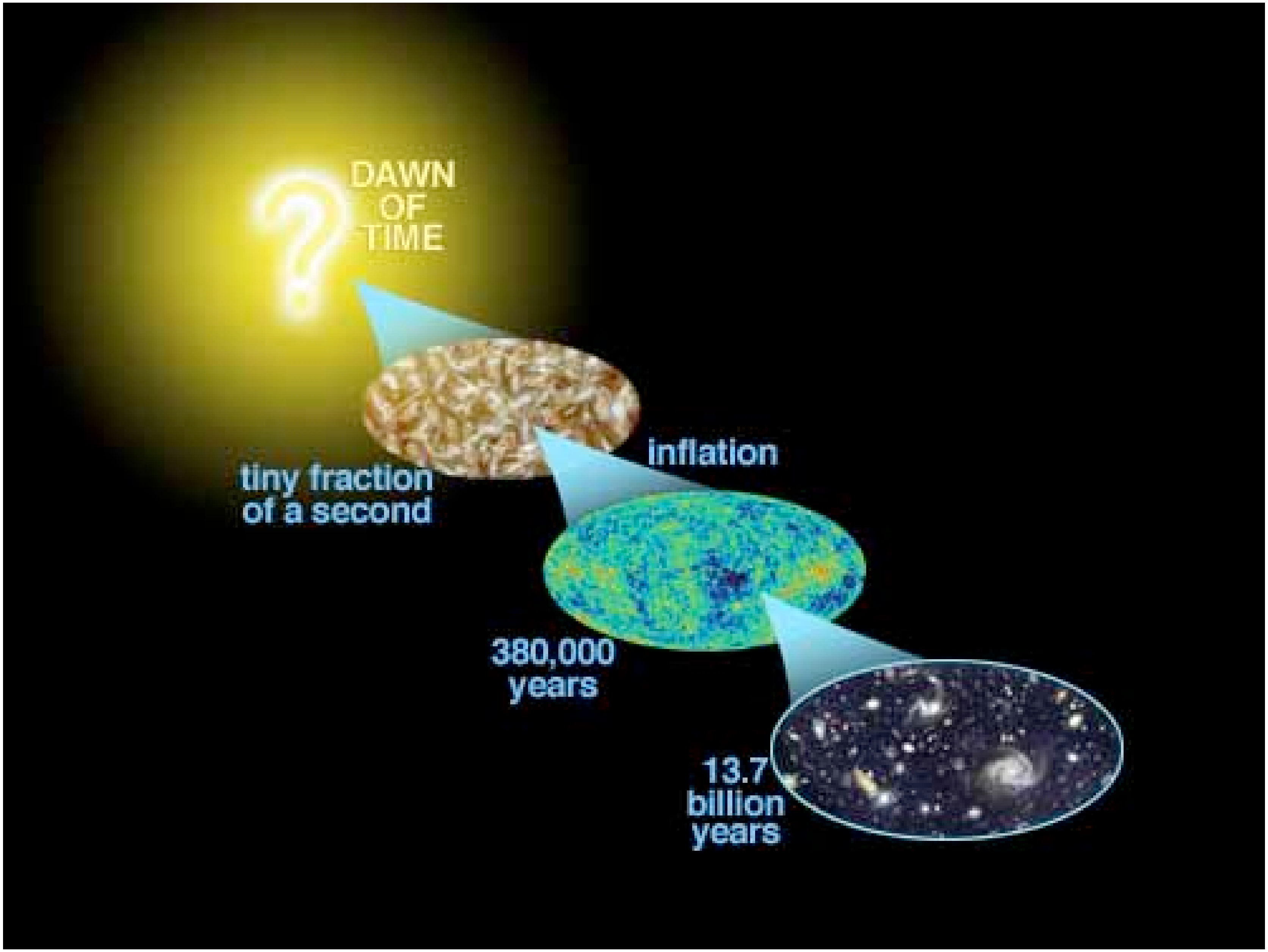

DAWN OF TIME
tiny fraction of a second
inflation
380,000 years
13.7 billion years

WMAP:five frequency maps

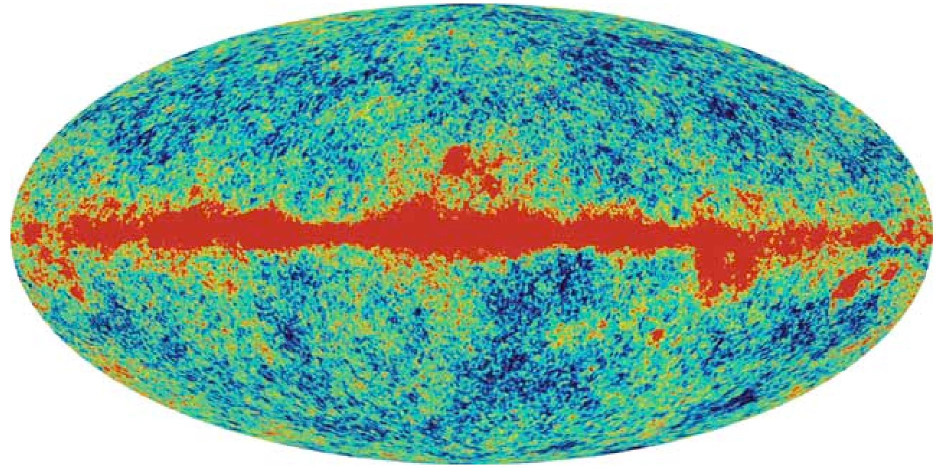

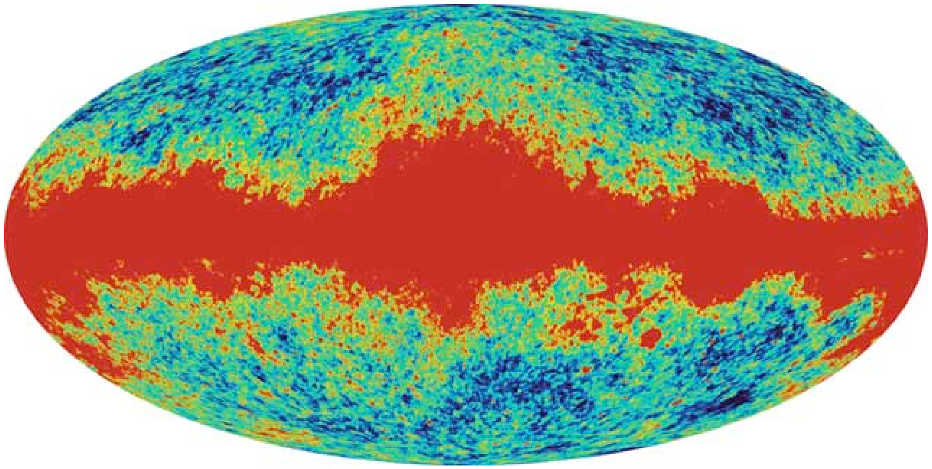

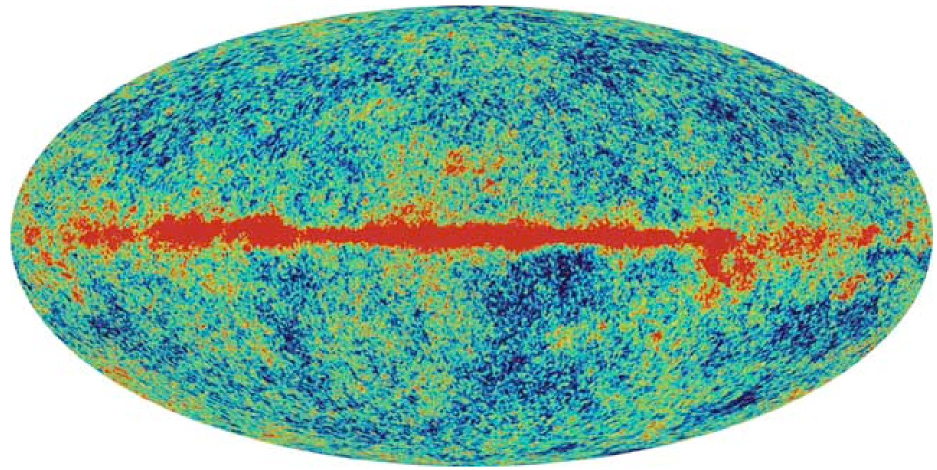

23, 33, 41, 61 and 93 GHz

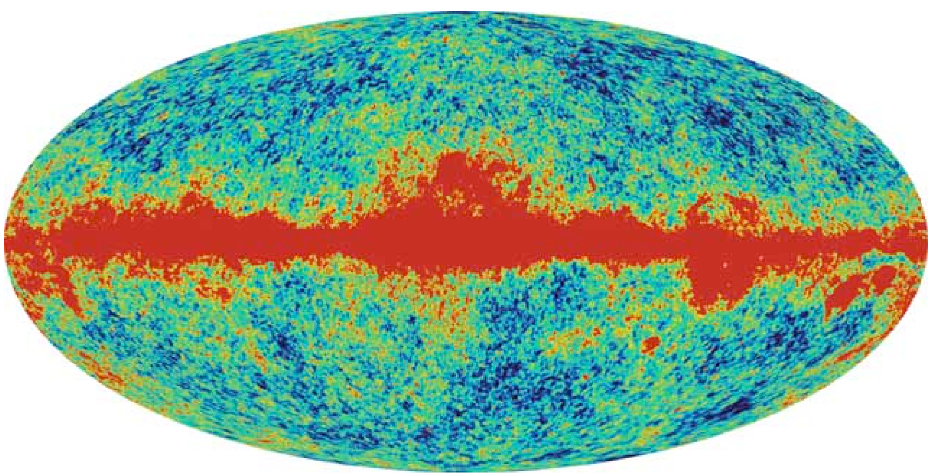

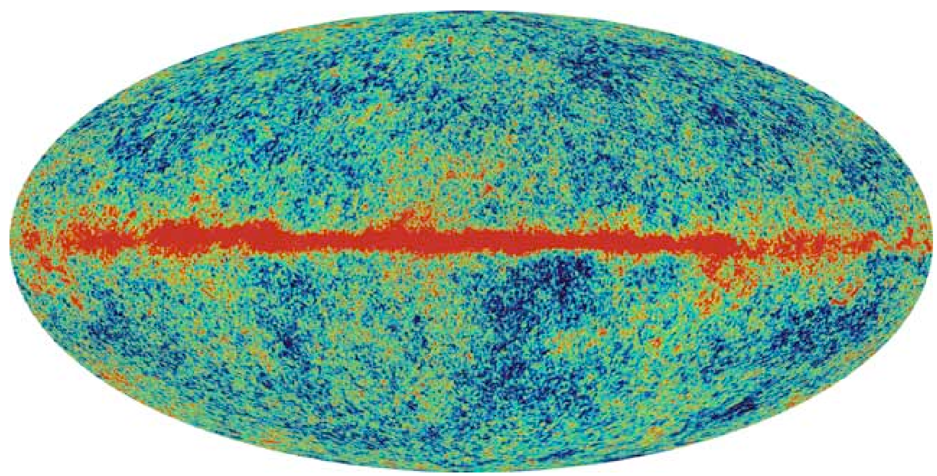

Healpix

K.M. Gorski et al., 1999, astro-ph/9812350,
http://www.eso.org/science/healpix

- Pixel = Rhombus
- Same Surfaces
- For a given latitude : regularly spaced
- Number of pixels: $12 \times (N_{sides})^2$
- Included in the software:
  - Anafast
  - Synfast

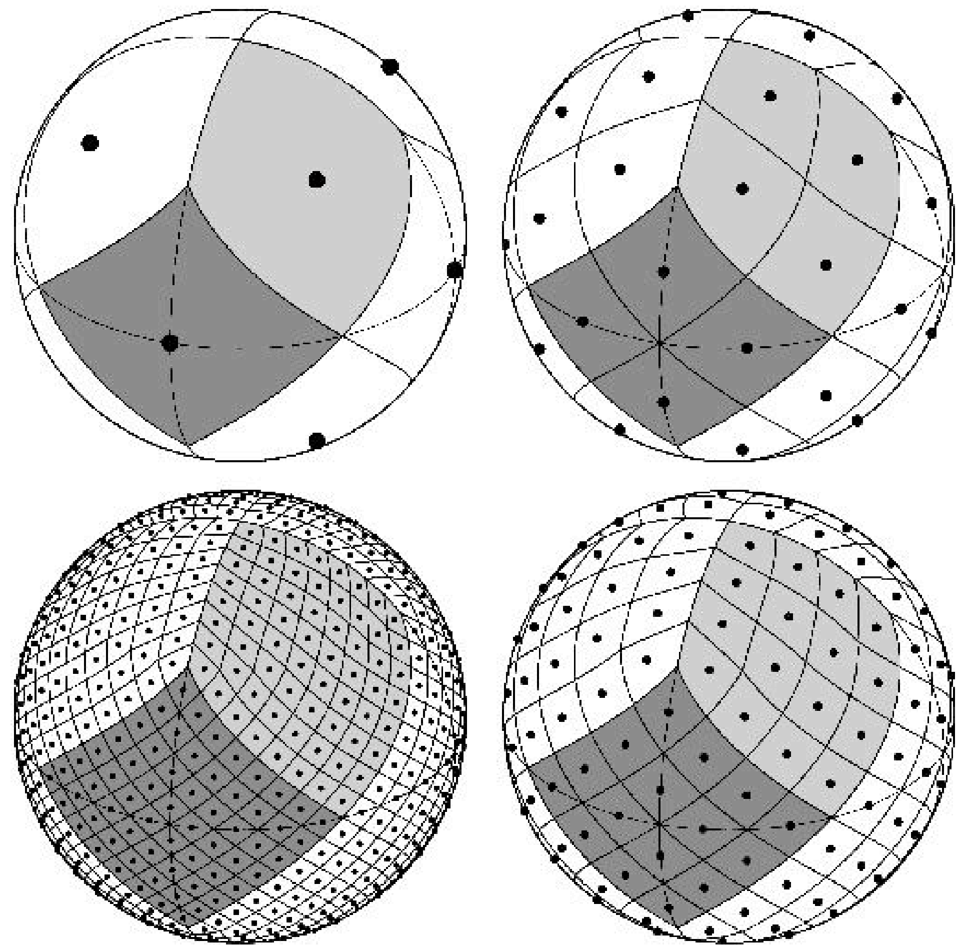

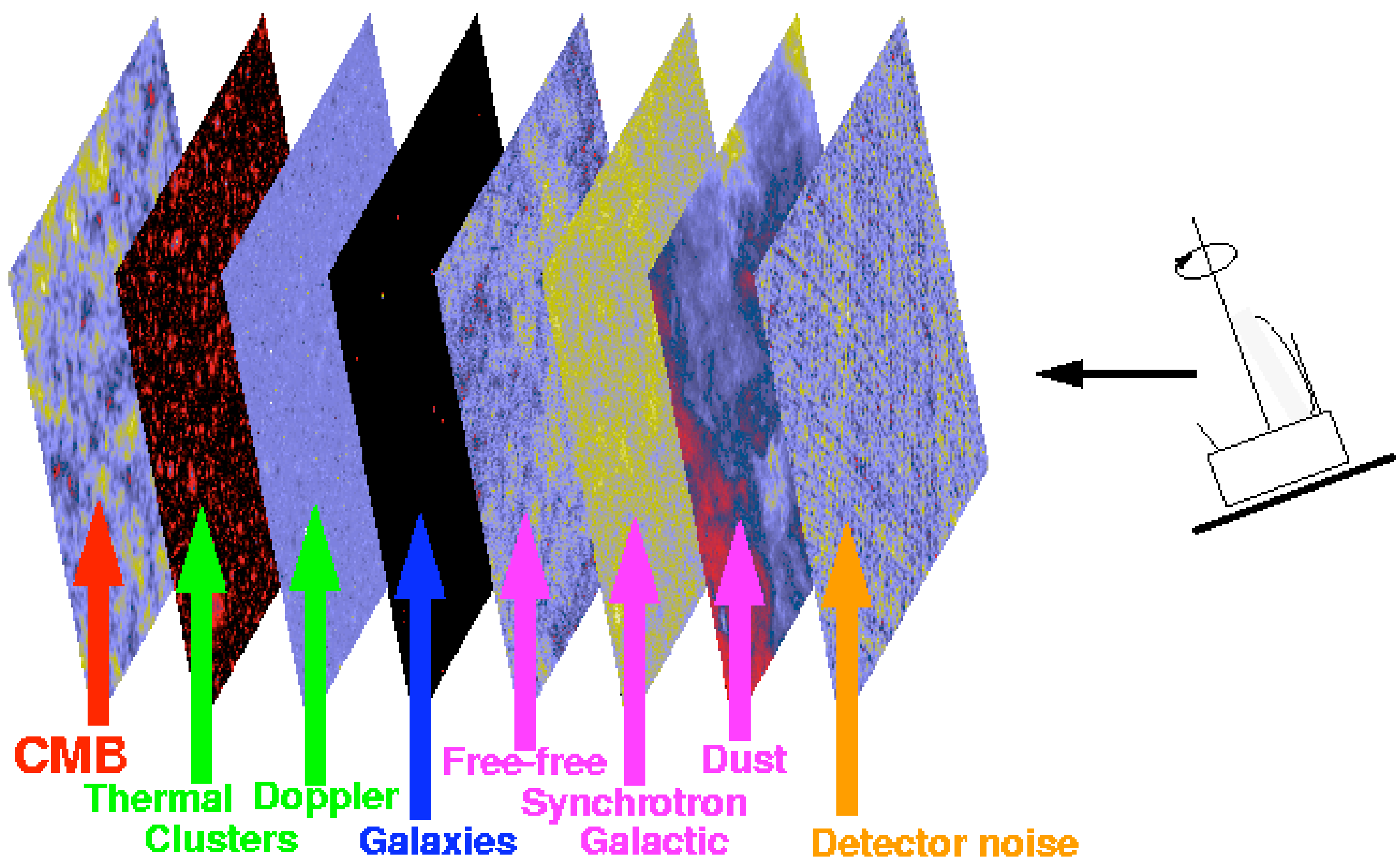

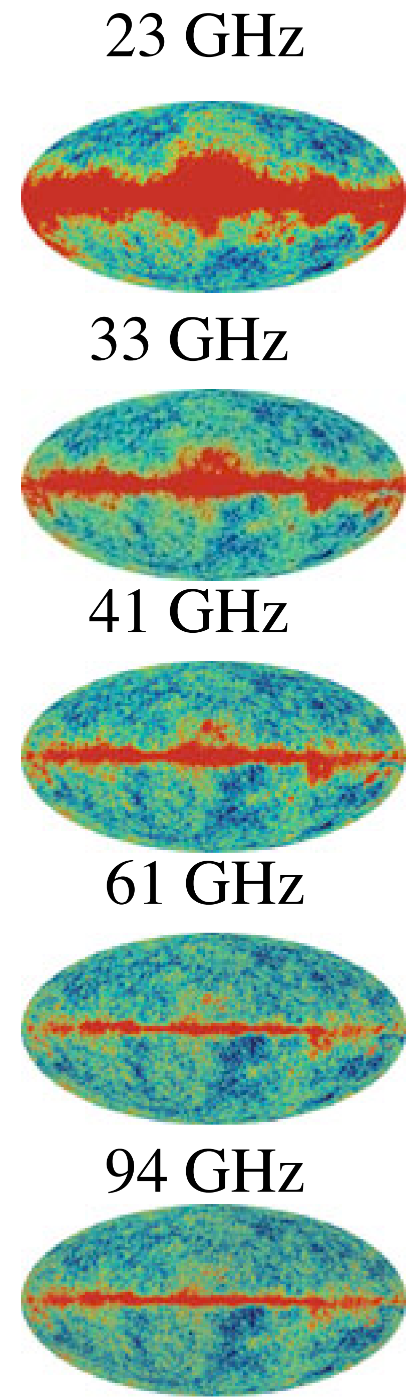

Synchrotron emission due to cosmic rays electrons accelerated into galactic magnetic fields

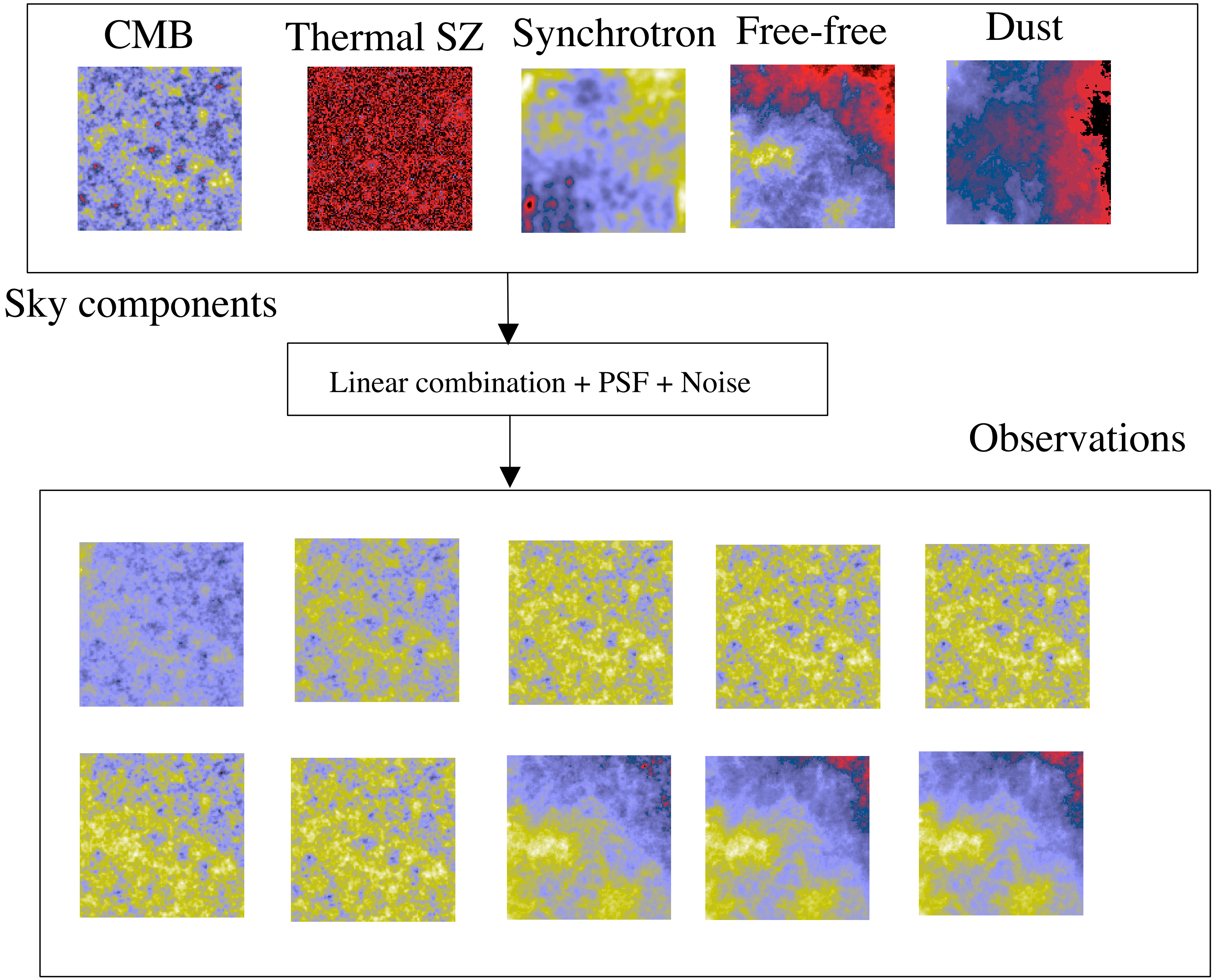
CMB
Thermal SZ
Synchrotron
Free-free
Dust
Sky components
Linear combination + PSF + Noise
Observations

WMAP derived sky maps

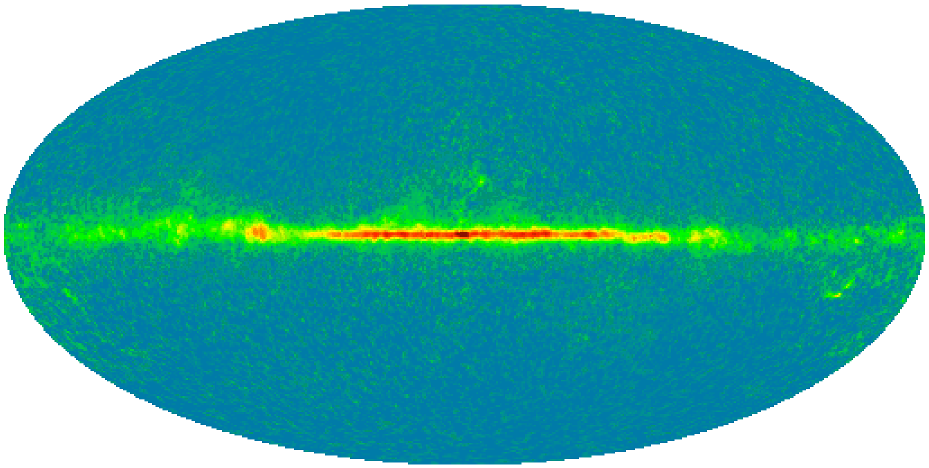

Dust map

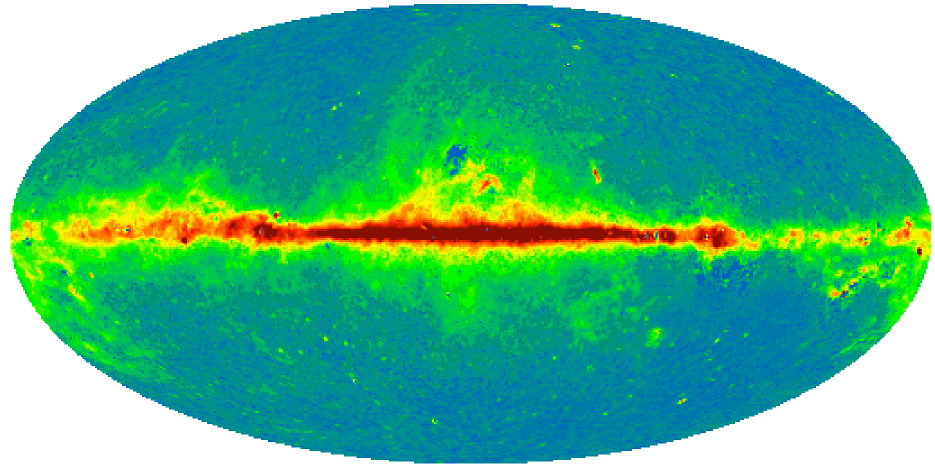

Synchrotron map

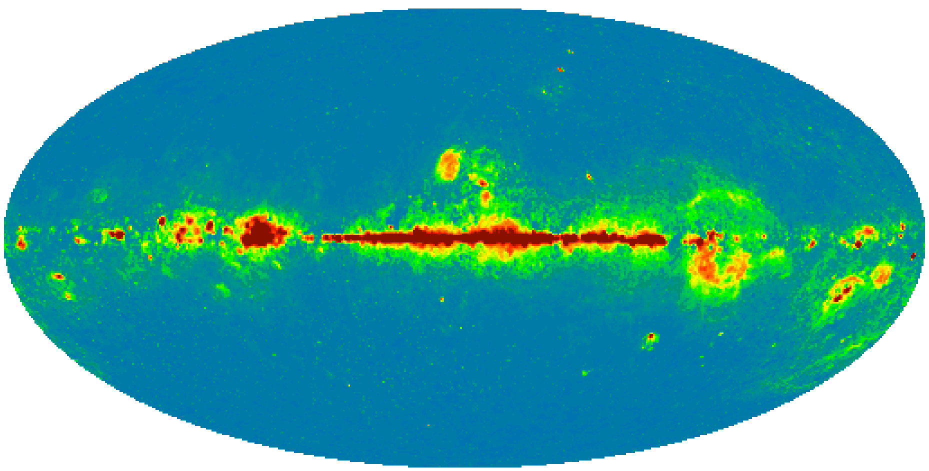

Free-free map

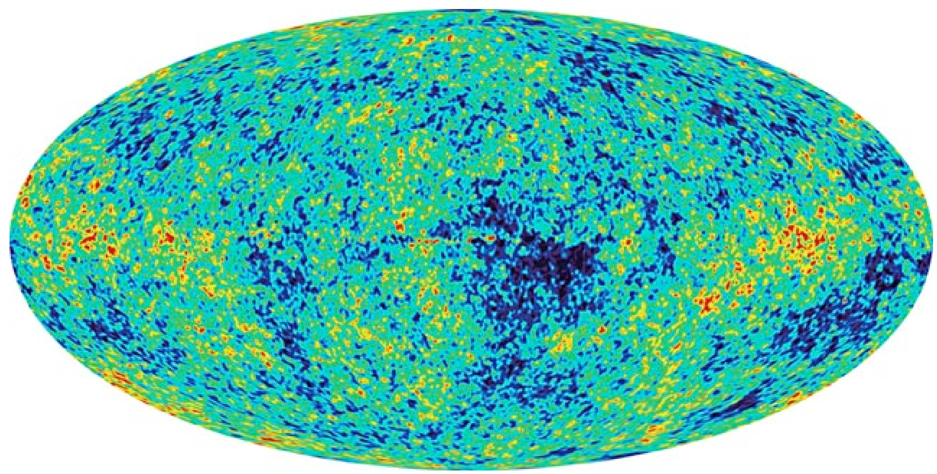

CMB map

The CMB exhibits Fluctuations

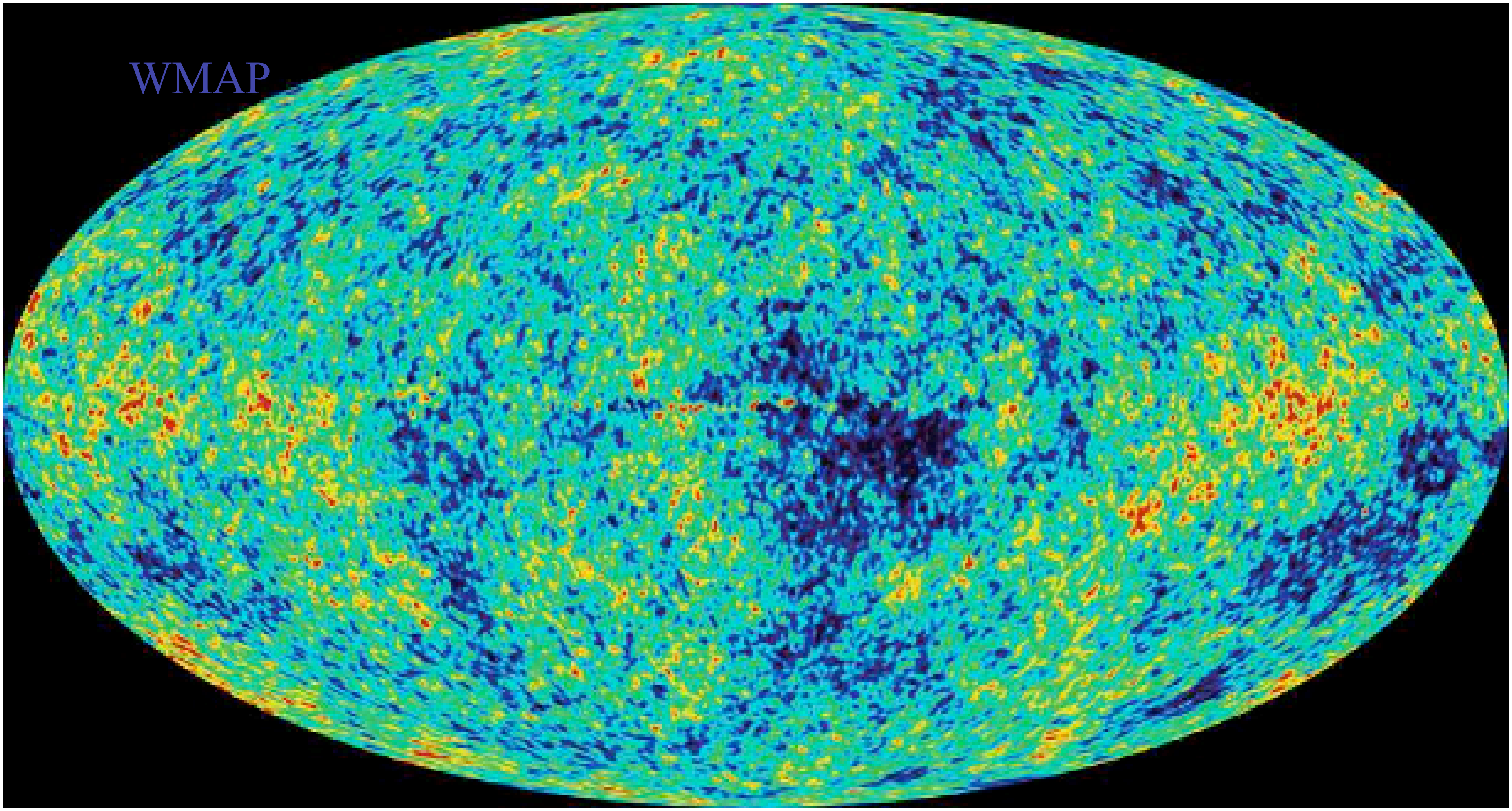

Power spectrum of WMAP

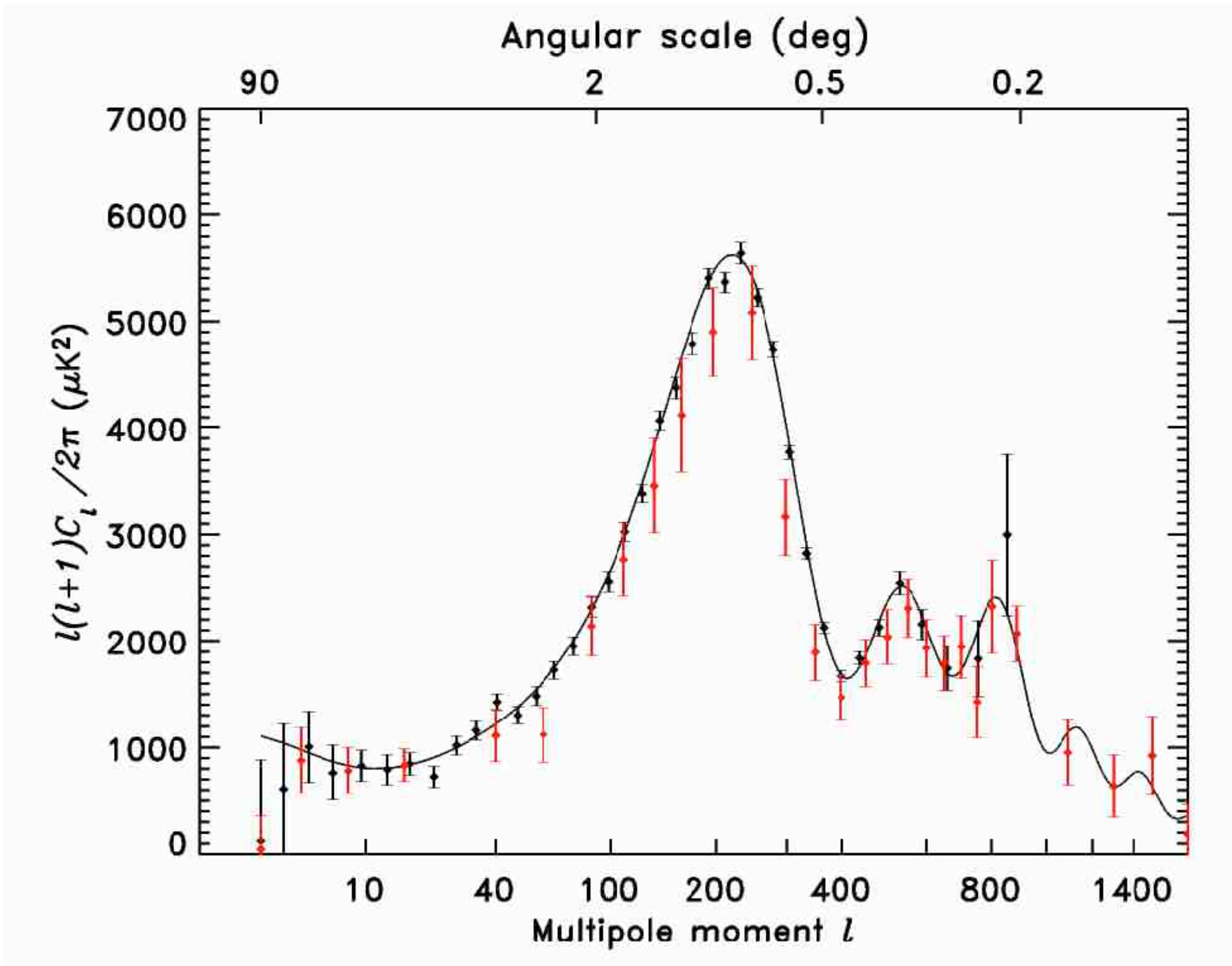

Remarkably consistent with earlier data

The Cosmic Microwave Background

• The power spectrum gives constraints on the geometry and the physical state of the Universe.

• It supports the hypothesis of a period of rapid expansion of the early Universe: the Inflationary period.

The Primary fluctuations

• This process causes randomly distributed seeds and Gaussian distributed fluctuations.

•At the end of this period, topological defects may occur that produce non-Gaussian fluctuations e.g. Cosmic Strings.

The Secondary fluctuations

The secondary fluctuations arise from the interaction of the CMB photons with the cluster of galaxies. It is the Sunyaev Zel'dovich (SZ) effect.

The Sunyaev Zel'dovich effect

- First predicted by the Russian scientists Sunyaev and Zel'dovich in 1969.
- Galaxy Clusters have hot gas
  - T_{gas}~10-100 million Kelvin
  - Electron scattering from nuclei produces X-rays, thermal bremsstahlung.
- Compton scattering occurs between CMB photons and the hot electrons.
  - ~1% of CMB photons will interact with the hot electrons
    - Energy will be transferred from the hot electrons to the low energy CMB photons, changing the shape of their intensity vs. frequency plot.
      - Measurements made at low frequencies will have a lower intensity, since photons which originally had these energies were scattered to higher energies. This distorts the spectrum by ~0.1%.
- Estimates of cosmological parameters (ie. H_o and Ω_b) can be made by combining these measurements.

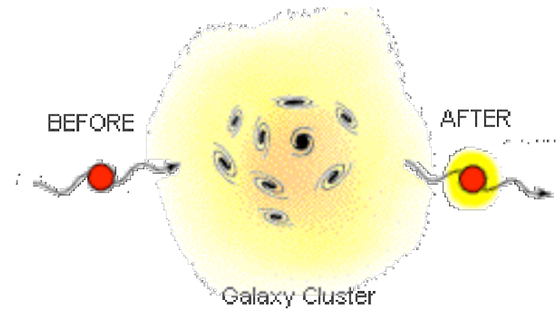

The SZ effect comes from the interaction of the cold CMB photons with the hot electrons (TSZ) of moving (KSZ) galaxy clusters

Detection of non-Gaussian Cosmological Signatures

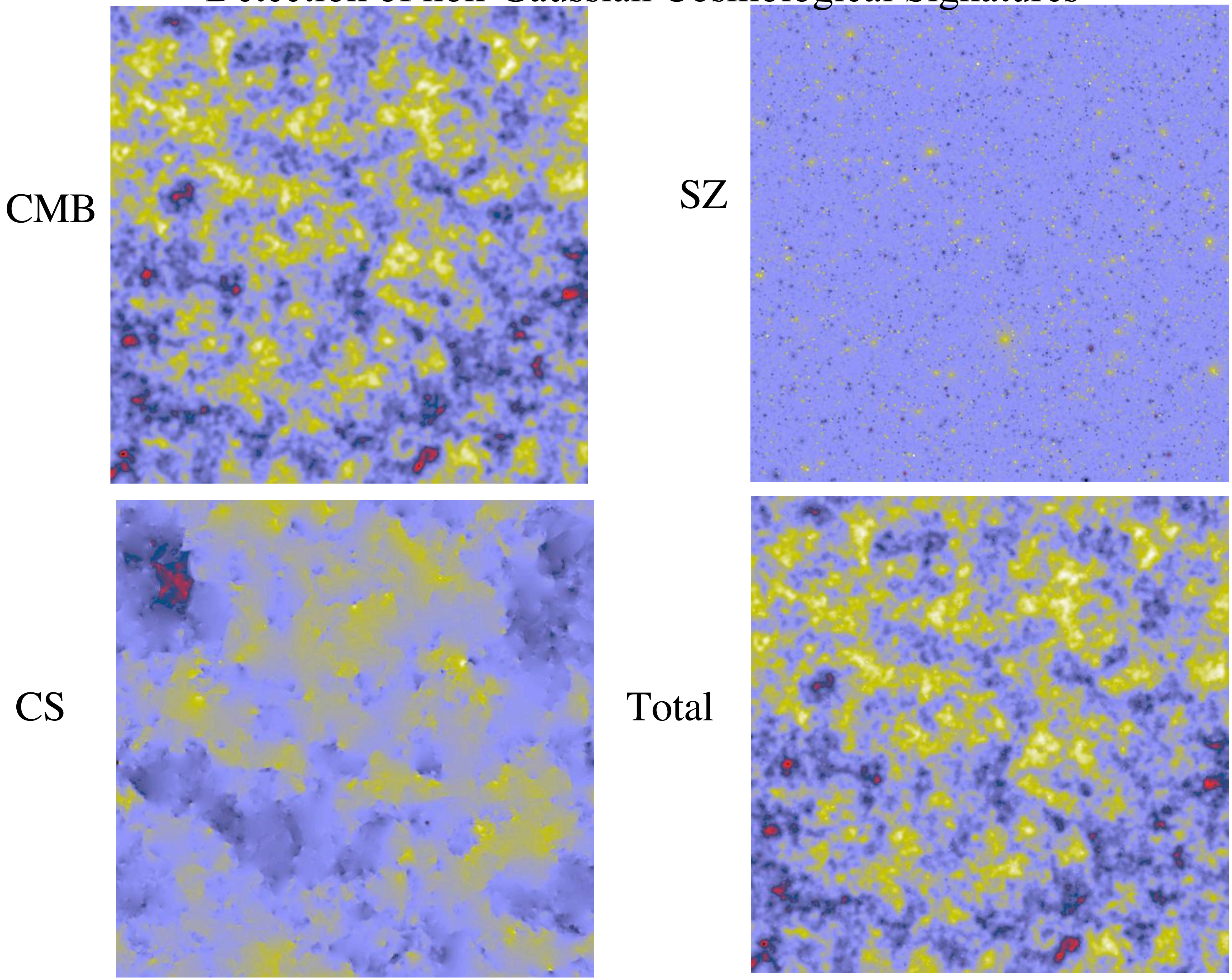

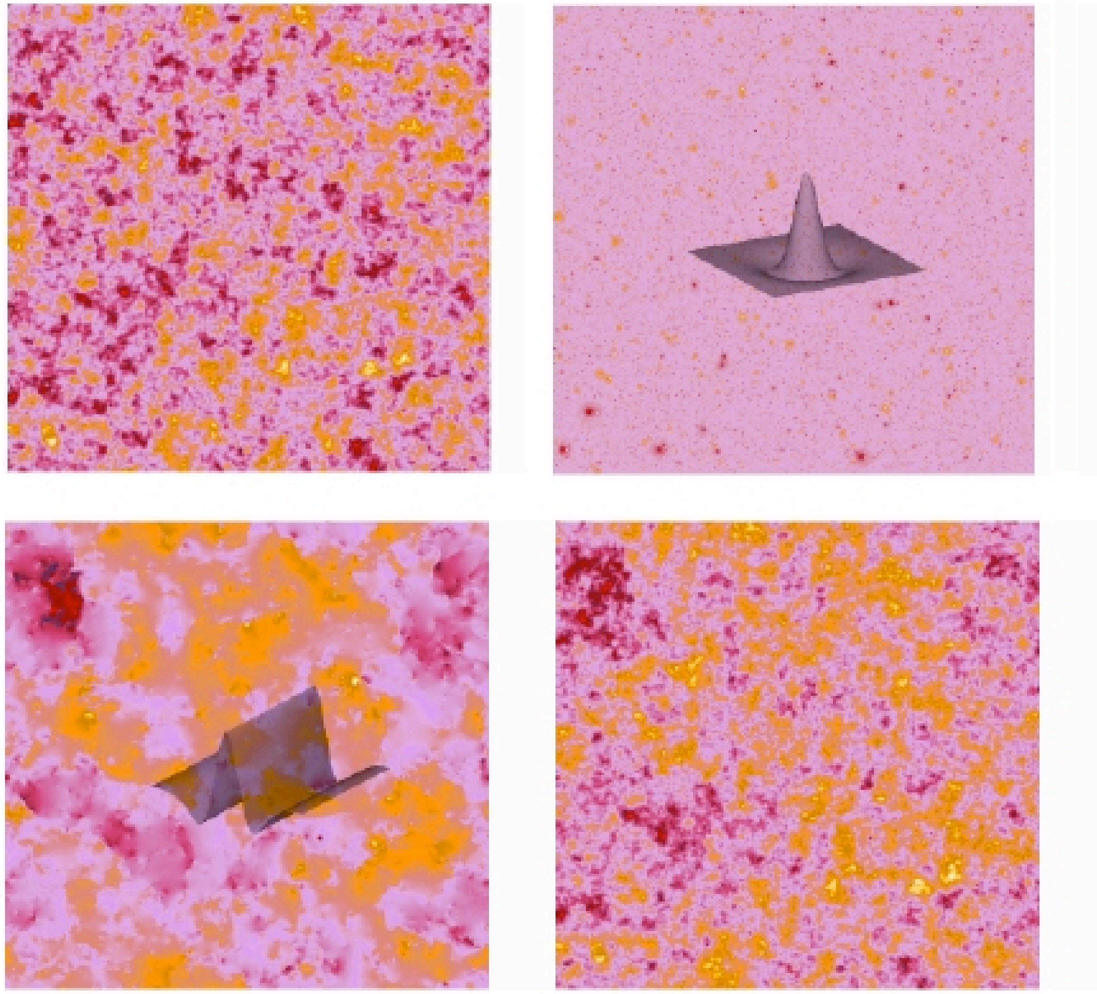

Multiscale Analysis of the CMB

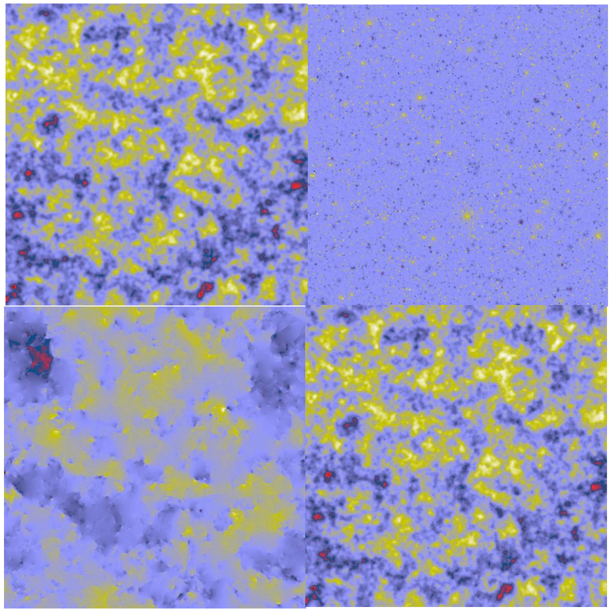

We have applied the following multiscale transforms

- Isotropic wavelet transform
- Bi-orthogonal wavelet transform
- Ridgelets (block size of 16 pixels)
- Ridgelets (block size of 32 pixels)
- Curvelets

On

1) 100 **CMB + KSZ** + 100 Gaussian realizations with the same power spectrum.

$$K_{CMB-SZ}(i,b) \Rightarrow K_{CMB-SZ}(b) = mean(K_{CMB-SZ}(1..100,b)), \overline{K}_{CMB-SZ}(b) = \frac{K_{CMB-SZ}(b)}{K_{CMB}(b)}$$

2) 100 **CMB + CS** + 100 Gaussian realizations with the same power spectrum

3) 100 **CMB + KSZ + CS** + 100 Gaussian realizations with the same power spectrum

We compare the normalized kurtosis for the three data set.

Results

- **Curvelets are NOT sensitive to KSZ but *are* sensitive to cosmic strings**

	Bi-orthogonal WT	Ridgelet	Curvelet
CMB+KSZ	1106.	0.1	10.12
CMB+CS	1813.	5.7	198.
CMB+CS+KSZ	1040.	5.9	165.

***Detecting cosmological non-Gaussian signatures by multi-scale methods**, Astron. and Astrophys., 416, 9--17, 2004* .

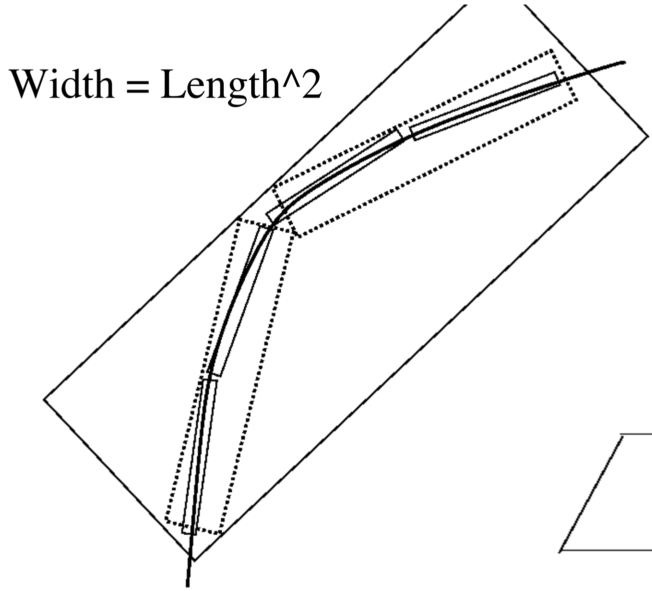

The Curvelet Transform

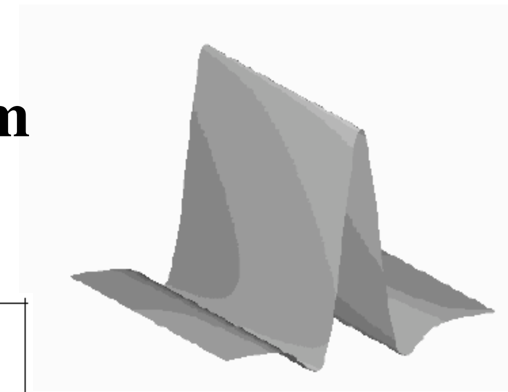

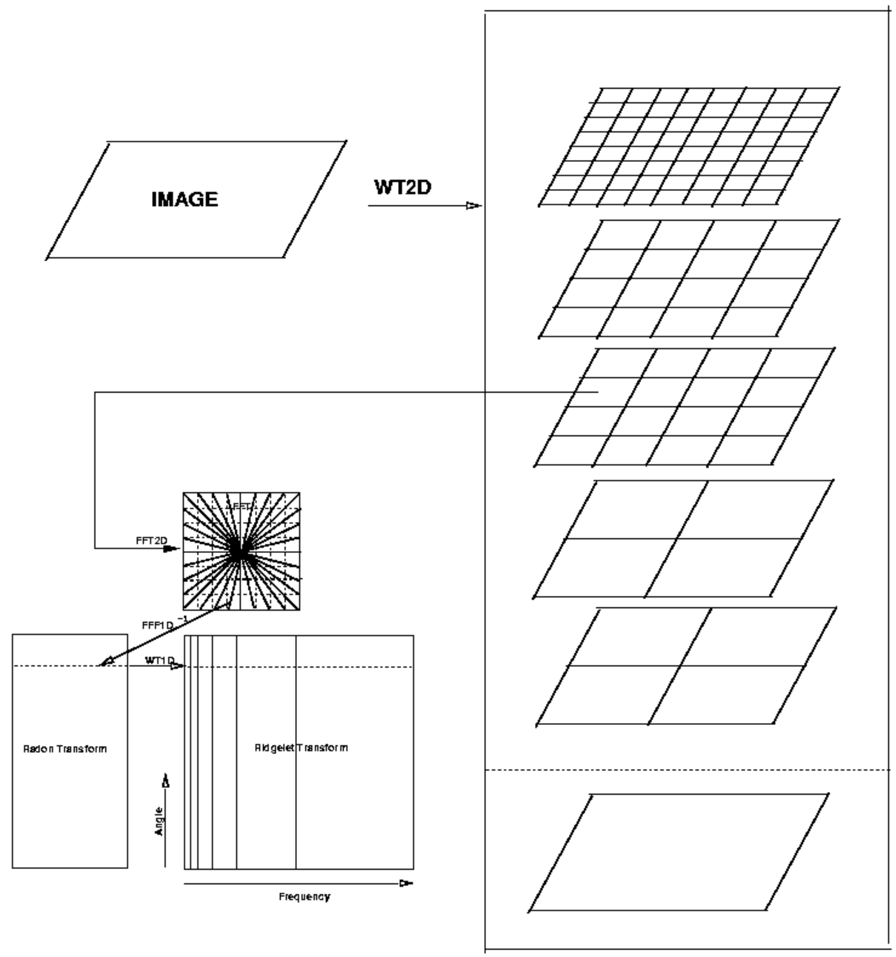

The Curvelet Transform for Image Denoising, *IEEE Transaction on Image Processing, 11, 6, 2002.*

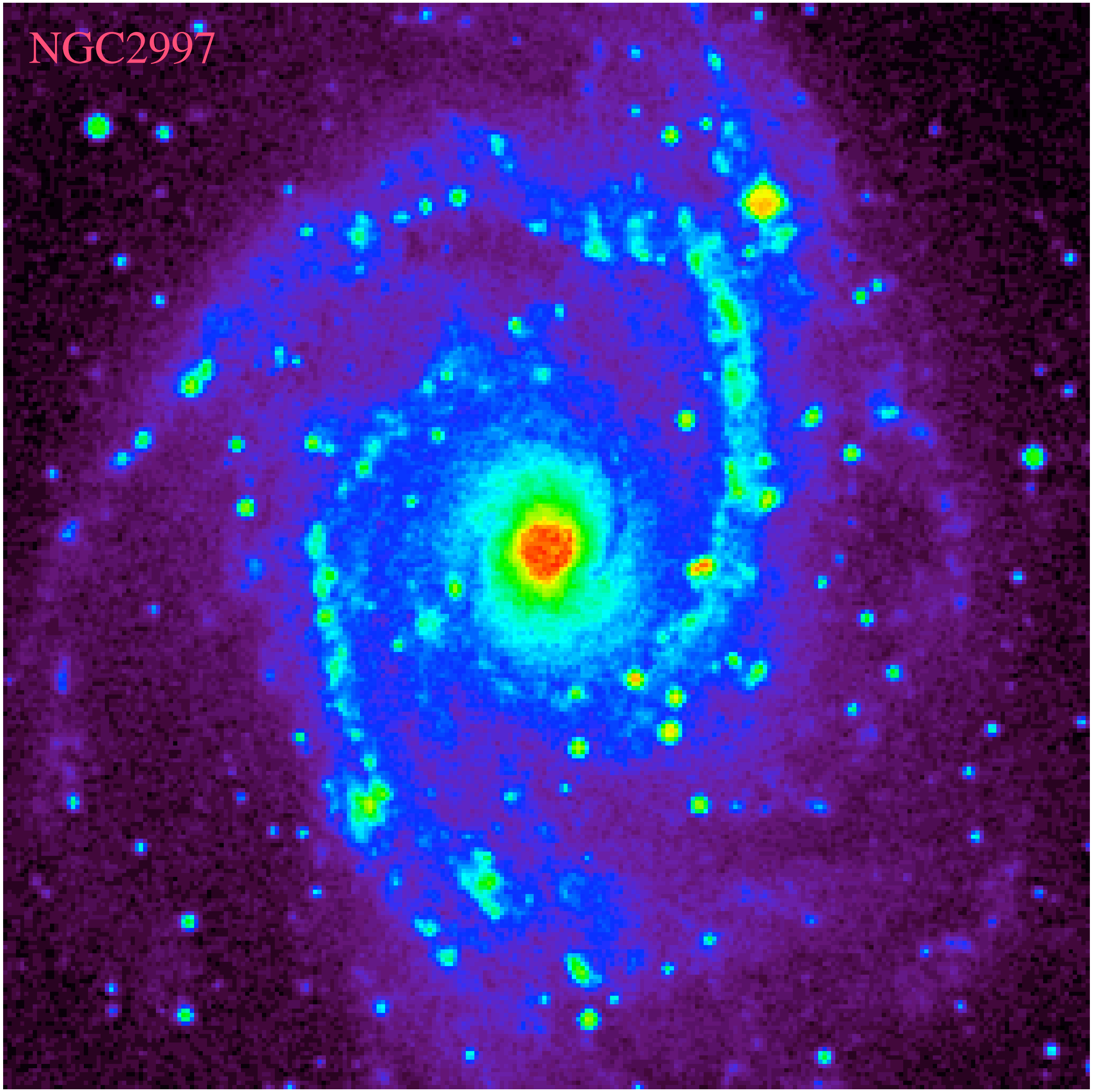
NGC2997

Undecimated Isotropic WT: $I(k,l) = c_{J,k,l} + \sum_{j=1}^{J} w_{j,k,l}$

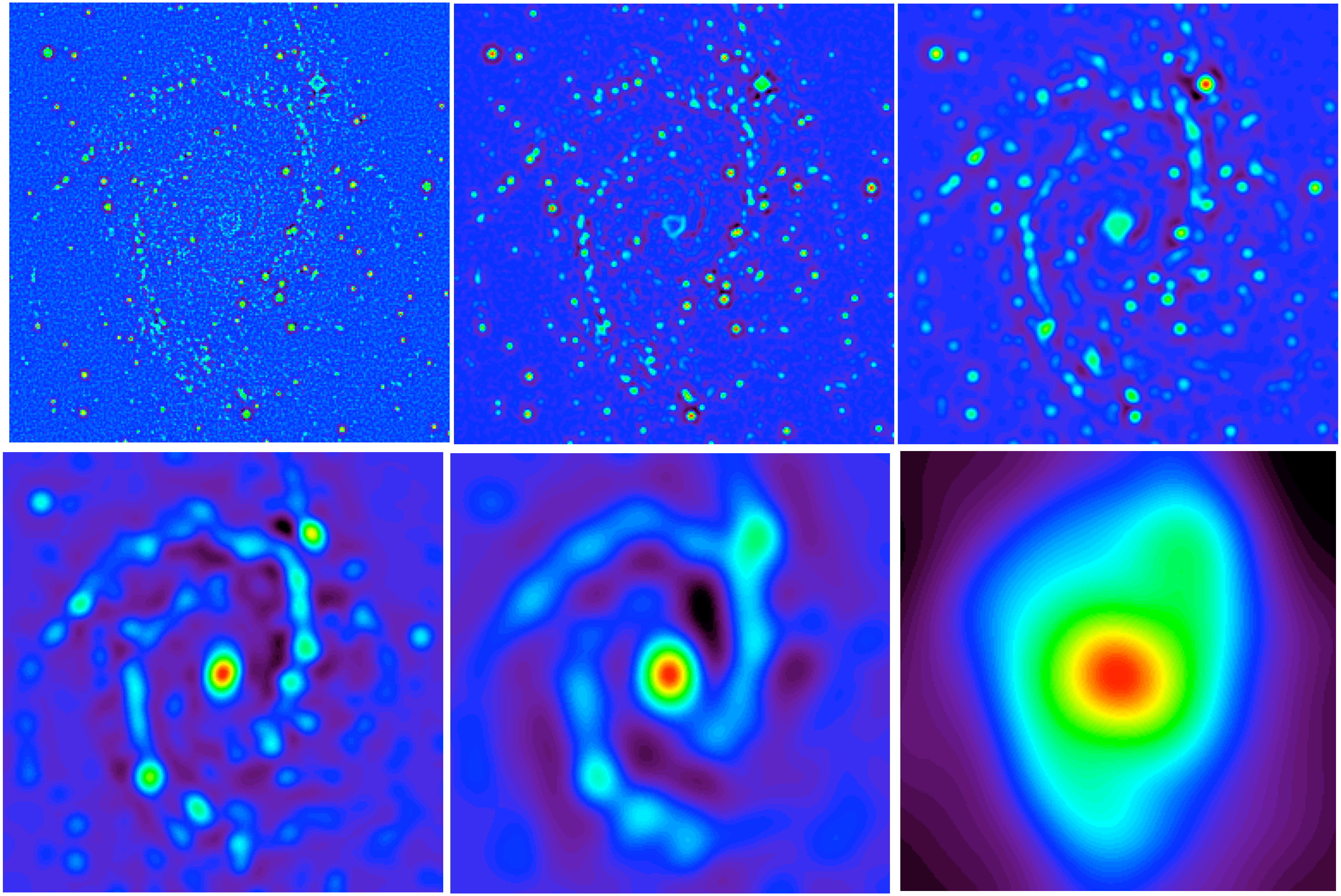

PARTITIONING

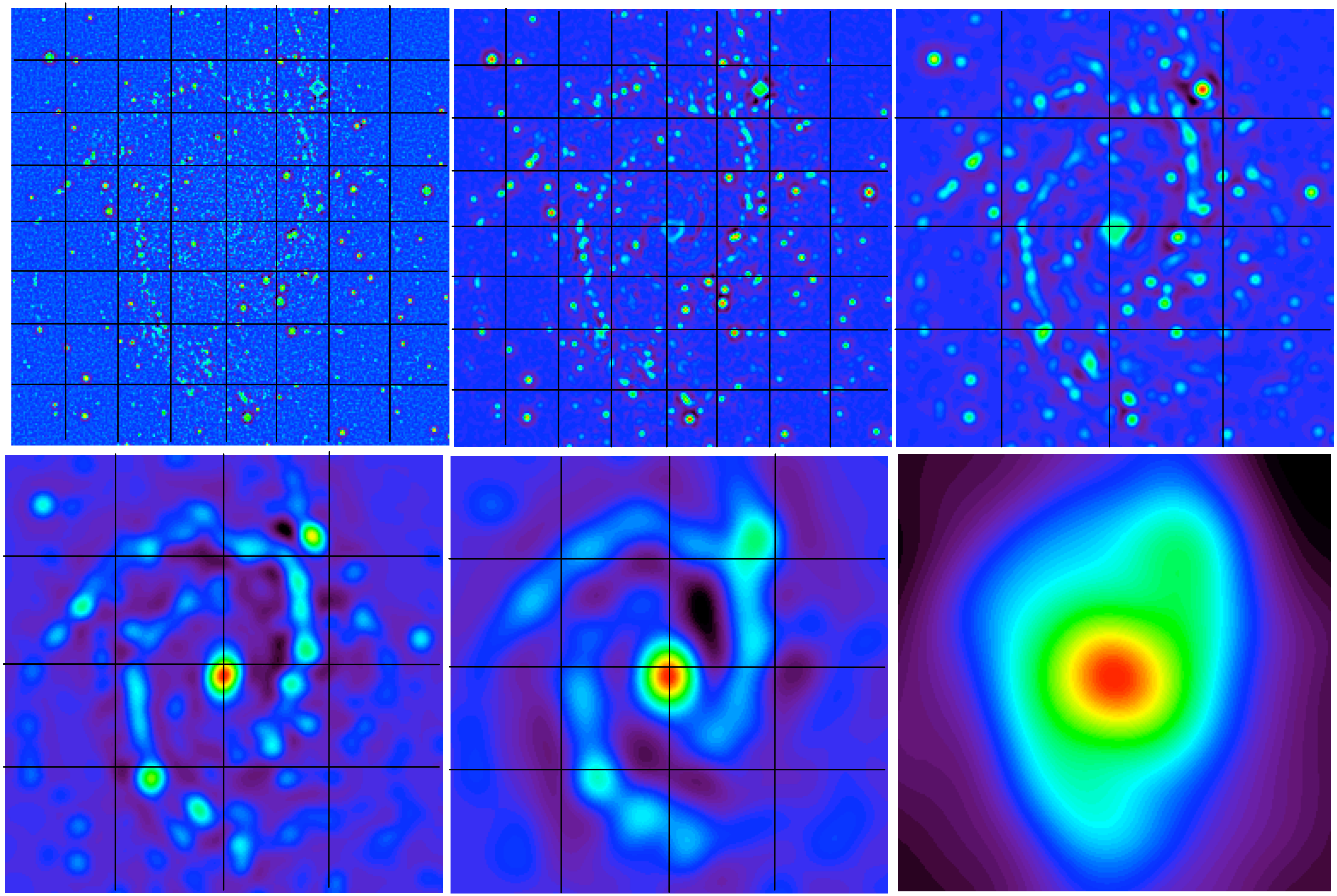

LOCAL RIDGELET TRANSFORM

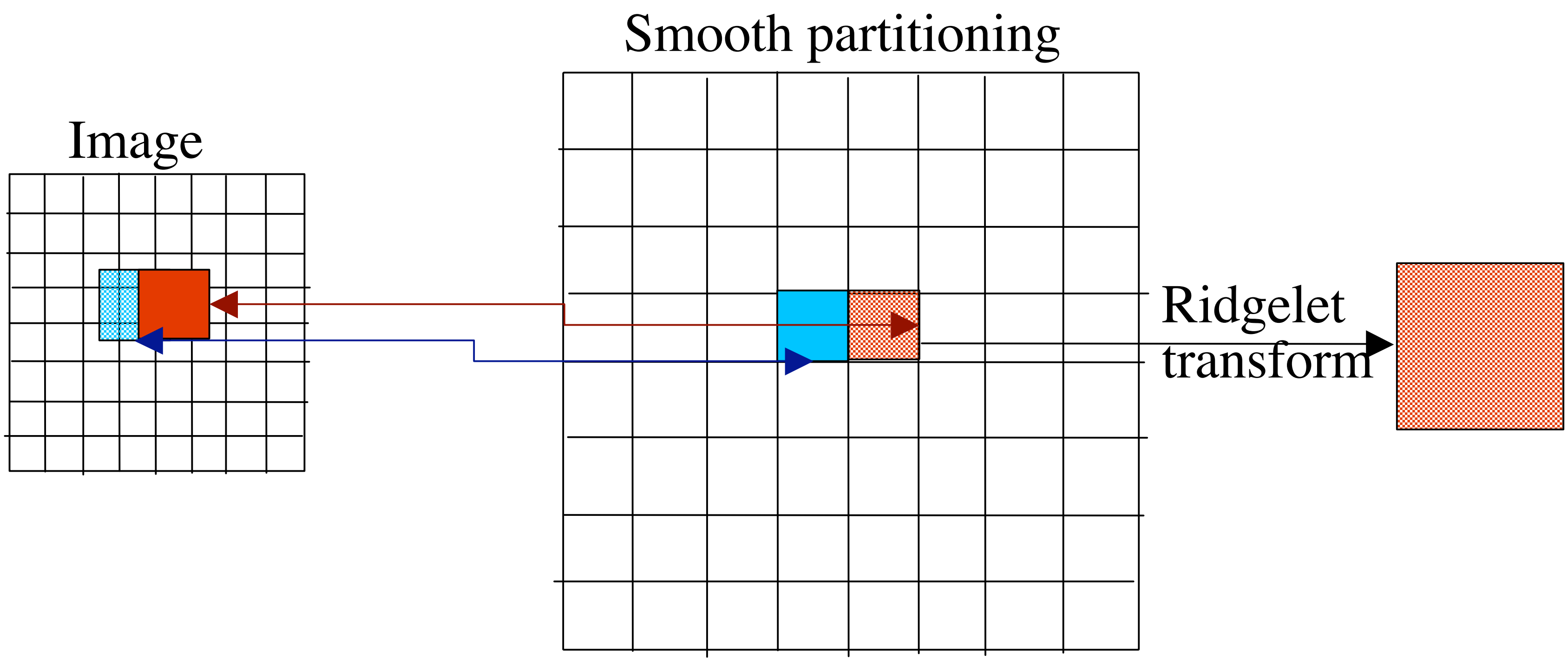

The partitioning introduces a redundancy, as a pixel belongs to 4 neighboring blocks.

The ridgelet coefficients of an object f are given by analysis of the Radon transform via: $R_f(a,b,\theta) = \int Rf(\theta,t)\psi(\frac{t-b}{a})dt$

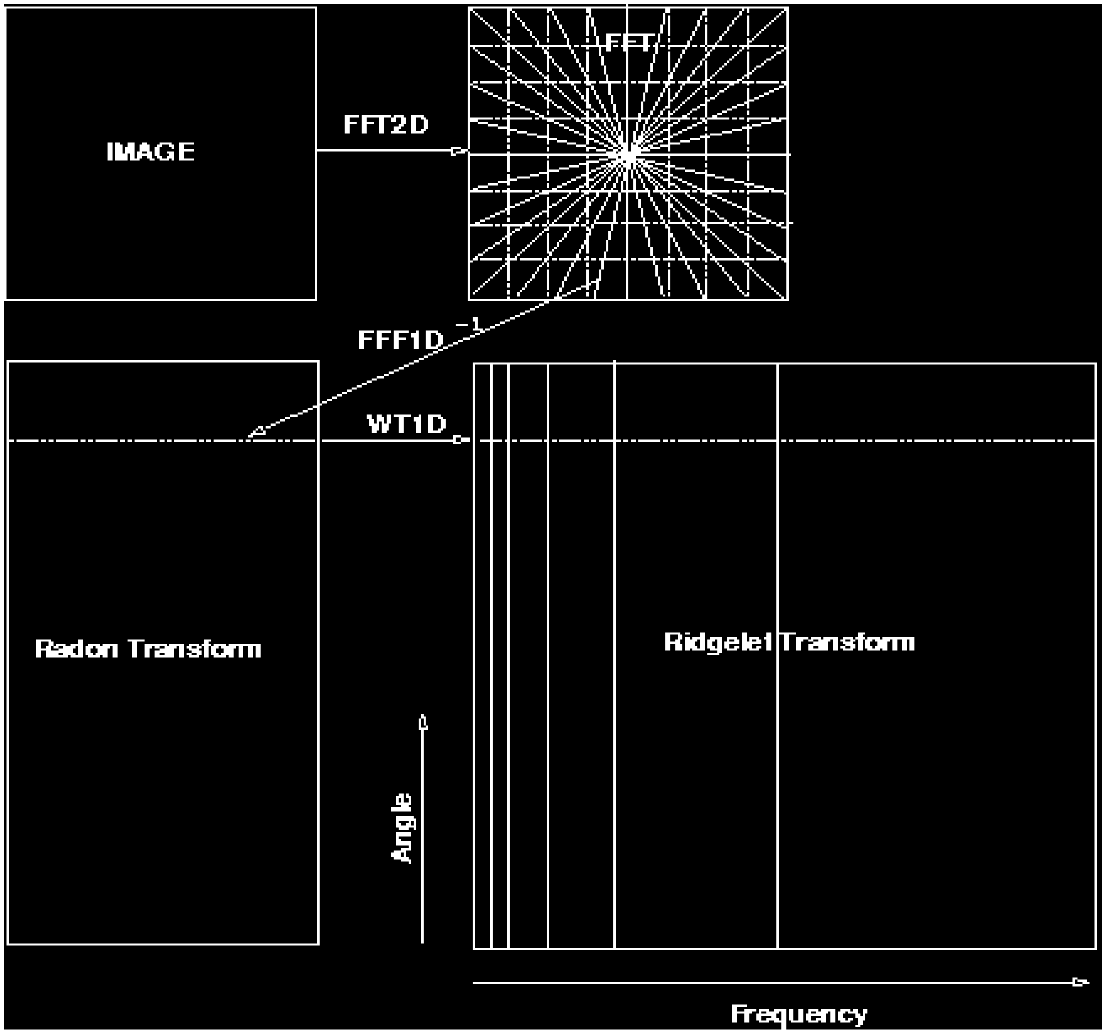

Curvelet Transform Implementations

1. CUR99 (Donoho, Candes, Duncan, 1999)
   Radon (linogram) + WT1D

2. CUR01 (Starck, Candes, Donoho, 2001)
   Radon (linogram) + WT1D

3. CUR03 (Candes, Donoho, 2003)
   In Fourier space using USFFT

4. CUR04 (Demanet, Candes, 2004)
   In Fourier space using warping

Slant Stack Radon Transform (Averbuch et al, 2001) or Linogram ?

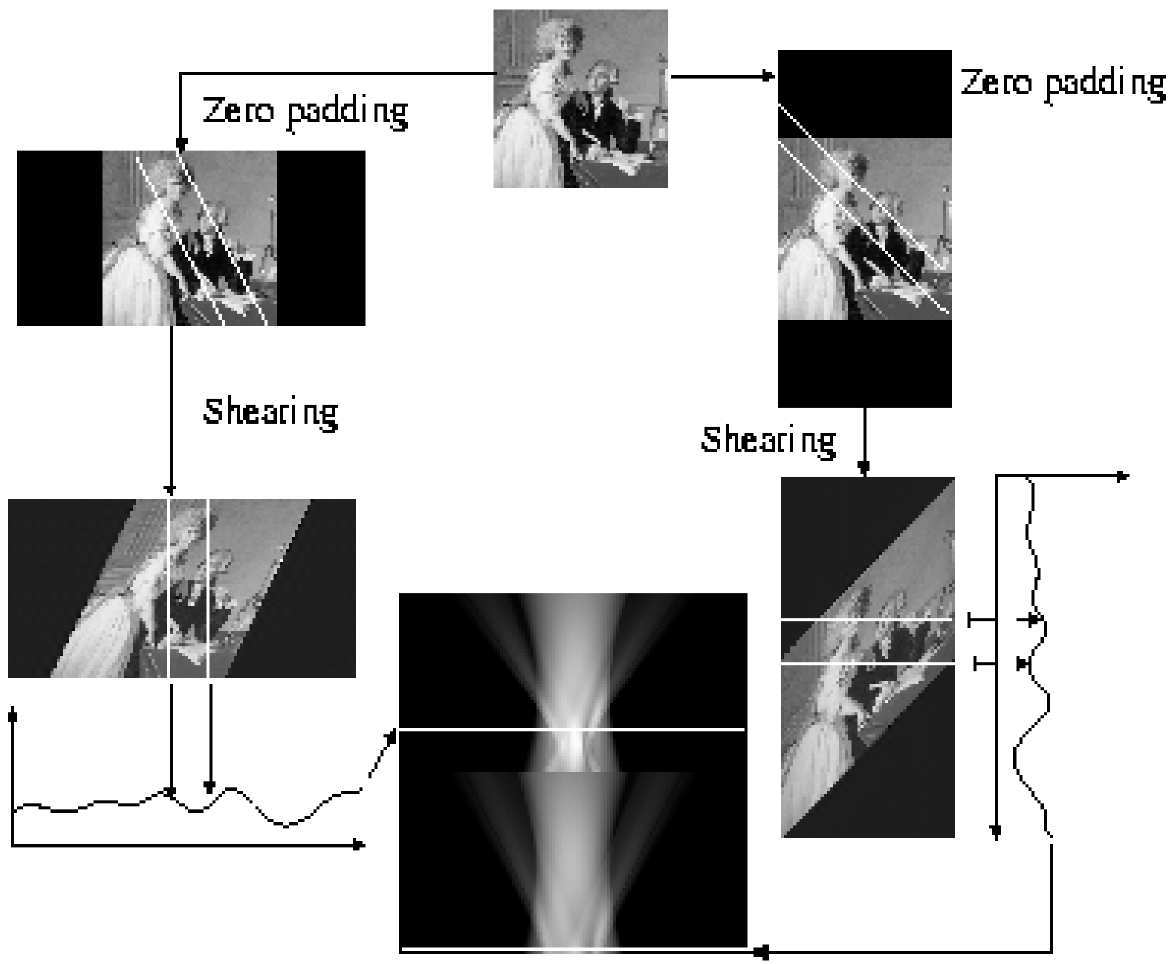

2Nx2N

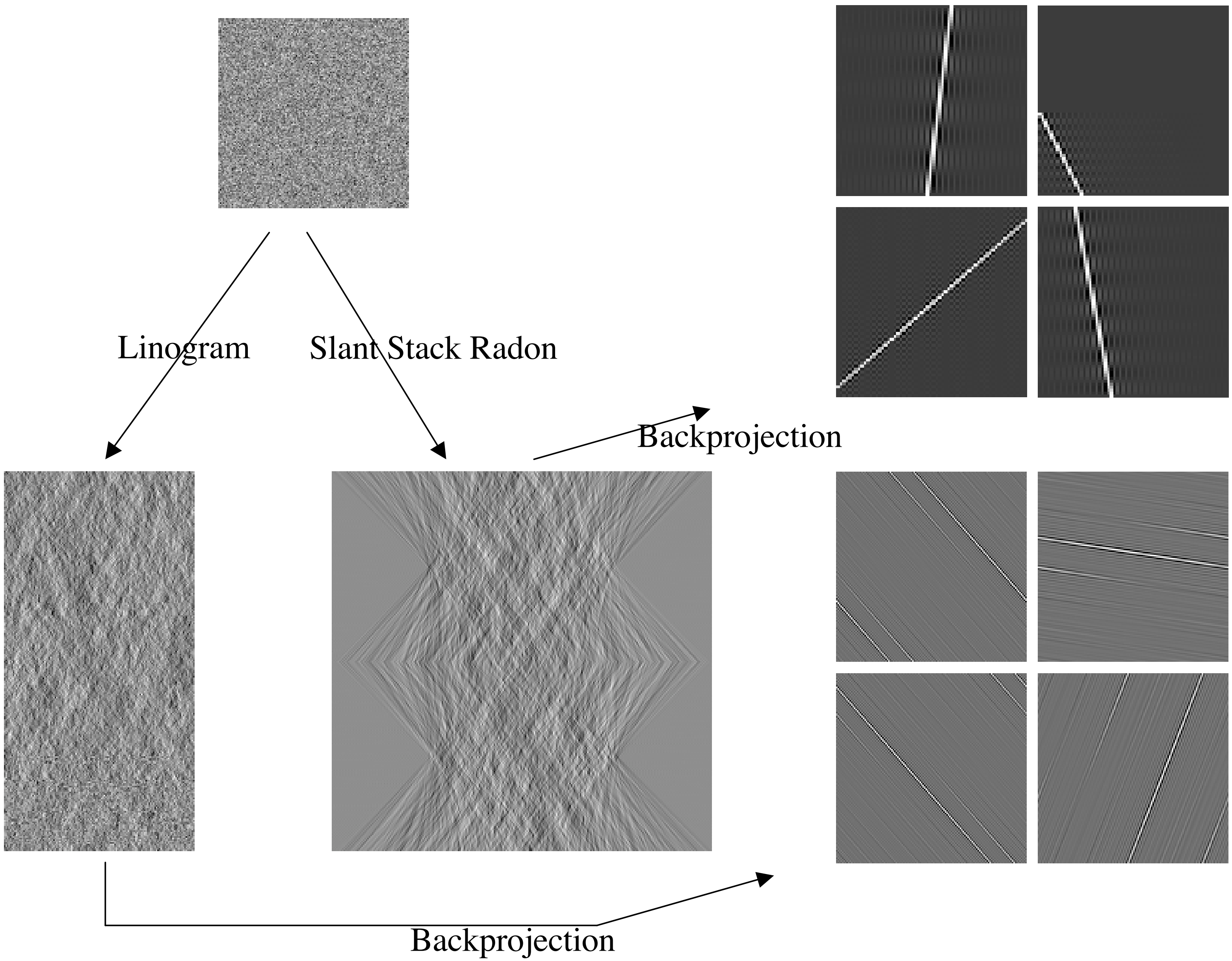
Linogram
Slant Stack Radon
Backprojection
Backprojection


CUR01+UWT, PSNR=32.10

Combined Filtering

***<u>Very High Quality Image Restoration</u>**, in Signal and Image Processing IX, San Diego, 1-4 August, 2001, Eds Laine, Andrew F.; Unser, Michael A.; Aldroubi, Akram, Vol. 4478, pp 9-19, 2001.*

$$\min \quad \text{Complexity\_penalty}(\tilde{s}), \qquad \text{subject to} \quad \tilde{s} \in C$$

Where C is the set of vectors which obey the linear constraints:

$$\tilde{s} > 0, \qquad \text{positivity constraint}$$

$$\left|\left(T_k \tilde{s} - T_k s\right)_l\right| \leq e, \quad if \left(T_k s\right)_l \quad \text{is significant}$$

The second constraint guarantees that the reconstruction will take into account any pattern which is detected by any of the K transforms.

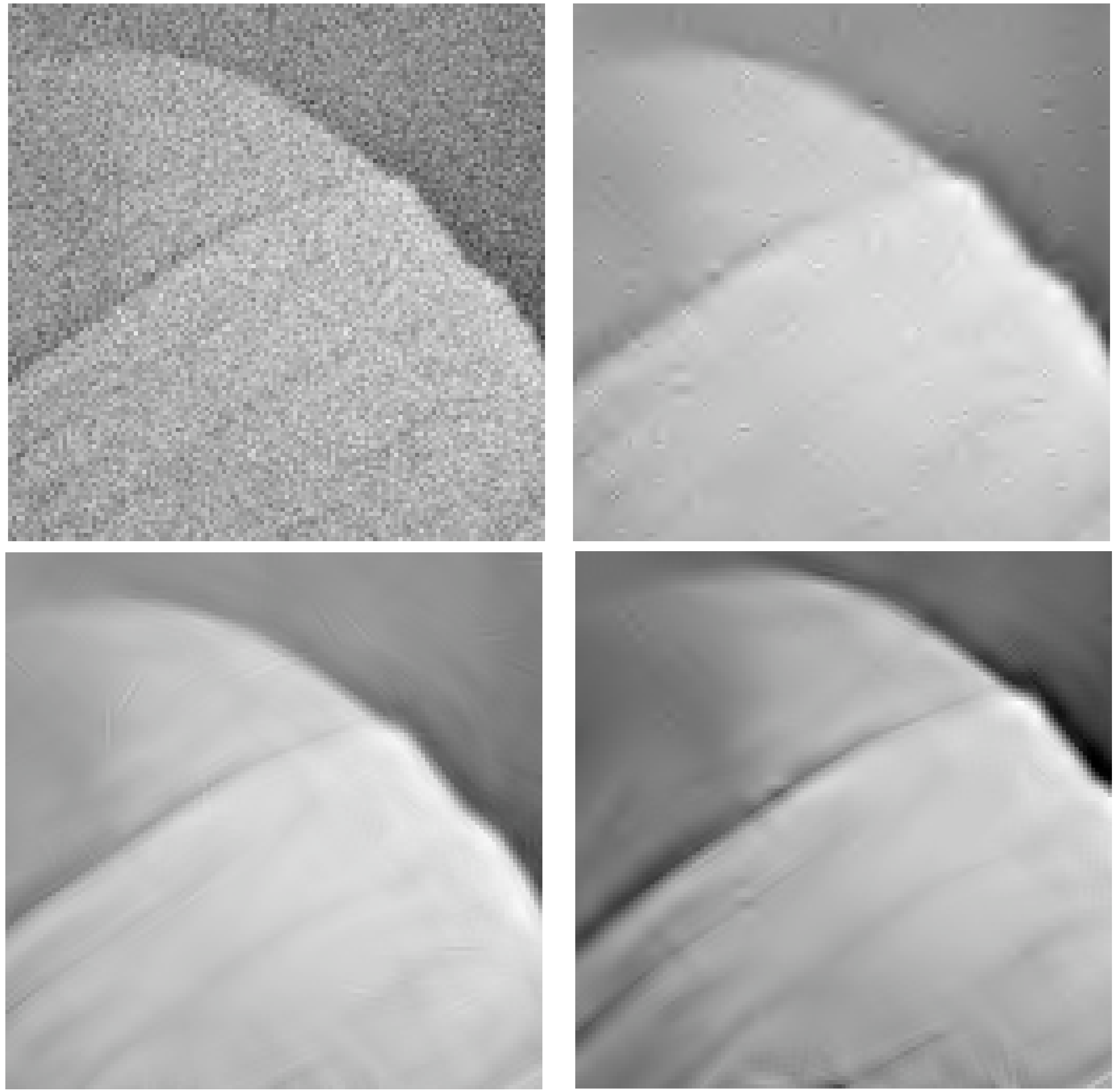

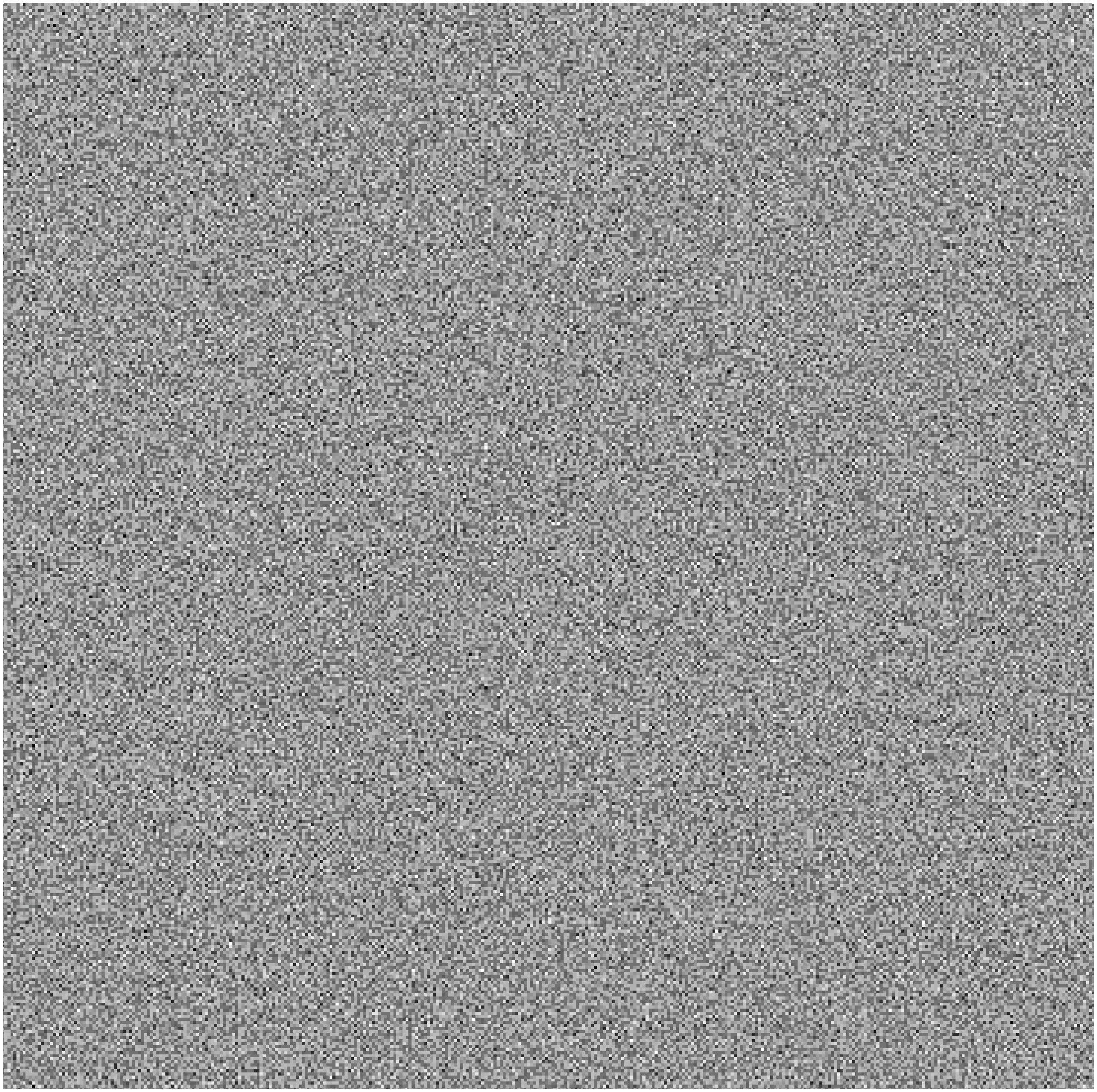

CUR01+UWT, PSNR=32.10

Simoncelli and Portilla (2003), PSNR=32.70

CUR01, PSNR=31.52

CUR01+SSR. PSNR=31.65

Notation: SSR: Slant Stack Radon
NOB: Non Overlapping Blocks

The improvement of the curvelet transform result when using SSR-CUR01 is only 0.1 dB on Lena, almost undistinguishable by eye, and the computation time is multiplied by 20.

If you don't use overlapping blocks, the SSR-CUR01-NOB is much better than CUR01-NOB, but SSR-CUR01-NO is still 5 times slower than CUR01 (WITH overlapping) and CUR01 is better by 0.5 dB than SSR-CUR01-NOB.

Conclusion: there is no need to use SSR in curvelet restoration applications.

PSNR

(=-10log10(Variance(Error)/255^2))

	Sigma=20	Sigma=42
DATA	22.09	15.66
UWT	31.36	28.66
CUR01	31.51	28.74
CUR01+ SSR	31.65	28.83
CUR03	30.90	27.90
CUR04	31.12	28.17
PORTILLA et al.	**32.70**	**28.99**
CUR01+UWT	32.11	28.90

Need for new representations on the sphere:

1) Isotropic Redundant WT on the Sphere

2) Ridgelets on the Sphere

3) Curvelet Transform on the Sphere

For restoration, we need an exact reconstruction

Wavelet on the Sphere

- P. Schroder and W. Sweldens (Orthogonal Haar WT), 1995.
- M. Holschneider, Continuous WT, 1996.
- **W. Freeden and T. Maier, OWT, 1998**.
- J.P. Antoine, Continuous WT, 1999.
- L. Tenerio, A.H. Jaffe, Haar Spherical CWT, (CMB), 1999.
- L. Cayon, J.L Sanz, E. Martinez-Gonzales, Mexican Hat CWT, 2001.
- J.P. Antoine and L. Demanet, Directional CWT, 2002.

Wavelet transform in the spherical harmonics space

We assume that

$$c_0(\theta, \phi) = c_{-1}(\theta, \phi) * \phi_{l_{max}}(\theta, \phi)$$

where $\phi_{l_{max}}$ is a low pass filter (scaling function) with a frequency cut-off l_{max}.
c_0 the input map, and c_{-1} an unknown function. A resolution level j is related to the HEALPix definition ($N_{side} = 2^j$).

The image at different resolutions is given by:

$$
\begin{aligned}
c_1(\theta,\phi) &= c_{-1}(\theta,\phi) * \phi_{l_{max}/2}(\theta,\phi) \\
c_2(\theta,\phi) &= c_{-1}(\theta,\phi) * \phi_{l_{max}/4}(\theta,\phi) \\
&\vdots \\
c_j(\theta,\phi) &= c_{-1}(\theta,\phi) * \phi_{l_{max}/2^j}(\theta,\phi)
\end{aligned}
$$

and the wavelet coefficients of the image are:

$$
\begin{aligned}
w_1(\theta,\phi) &= c_{-1}(\theta,\phi) * \psi_1(\theta,\phi) \\
w_2(\theta,\phi) &= c_{-1}(\theta,\phi) * \psi_2(\theta,\phi) \\
&\vdots \\
w_j(\theta,\phi)) &= c_{-1}(\theta,\phi) * \psi_j(\theta,\phi)
\end{aligned}
$$

where ψ_j is the wavelet function at scale j.

Choice of Scale Function and Wavelet Function

We define $\phi_{l_{max}}$ in the Spherical Harmonics space as a B-spline function. The B-spline function is

$$B(x) = \frac{1}{12}(\mid x-2\mid^3 - 4\mid x-1\mid^3 + 6\mid x\mid^3 - 4\mid x+1\mid^3 + \mid x+2\mid^3)$$

and the scaling function $\phi_{l_{max}}$ is:

$$\hat{\phi}_{l_{max}}(l,m) = \frac{3}{2}B(\frac{l}{l_{max}})$$

The wavelet can be chosen as the difference between two resolutions:

$$\psi_j(\theta,\phi) = \phi_{l_{max}/2^{j-1}}(\theta,\phi) - \phi_{l_{max}/2^j}(\theta,\phi)$$

From one resolution to the next one

The image at the first scale is given by: $c_0(\theta,\phi) = c_{-1}(\theta,\phi) * \phi_{l_{max}}(\theta,\phi)$, which gives in space of spherical harmonics (as $\phi_{l_{max}}$ is azimuthally symmetric):

$$\hat{c_0}(l,m) = \sqrt{\frac{2l+1}{4\pi}}\hat{c}_{-1}(l,m)\hat{\phi}_{l_{max}}(l,m)$$

The coefficients which allow us to go from one resolution to the next one are obtained with the discrete filters h and h:

$$\hat{h}(l,m) = \begin{cases} \frac{\hat{\phi}_{l_{max}}(2l,m)}{\hat{\phi}_{l_{max}}(l,m)} & \text{if } l < l_{max} \\ 0 & \text{otherwise} \end{cases}$$

$$\hat{g}(l,m) = \begin{cases} \frac{\hat{\psi}_{1}(2l,m)}{\hat{\phi}_{l_{max}}(l,m)} & \text{if } l < l_{max} \\ 0 & \text{otherwise} \end{cases}$$

We have:

$$\begin{aligned} \hat{c}_{j+1}(l,m) &= \hat{c}_j(l,m)\hat{h}(2^j l,m) \\ \hat{w}_{j+1}(l,m) &= \hat{c}_j(l,m)\hat{g}(2^j l,m) \end{aligned}$$

The cut-off frequency is reduced by a factor 2 at each step.

Reconstruction

If the wavelet is the difference between two resolutions, an evident reconstruction for a wavelet transform $\mathcal{W} = \{w_1, \dots, w_J, c_J\}$ is:

$$c_0(\theta, \phi) = c_J(\theta, \phi) + \sum_j w_j(\theta, \phi)$$

An alternative is to use the conjugate filters defined by

$$\begin{aligned} \hat{\tilde{h}} &= \hat{h}^* / (\mid \hat{h} \mid^2 + \mid \hat{g} \mid^2) \\ \hat{\tilde{g}} &= \hat{g}^* / (\mid \hat{h} \mid^2 + \mid \hat{g} \mid^2) \end{aligned}$$

And the reconstruction is obtained by:

$$\hat{c}_j(l, m) = \hat{c}_{j+1}(l, m) \hat{\tilde{h}}(l_{max}/2^j, m) + \hat{w}_{j+1}(l, m) \hat{\tilde{g}}(l_{max}/2^j, m)$$

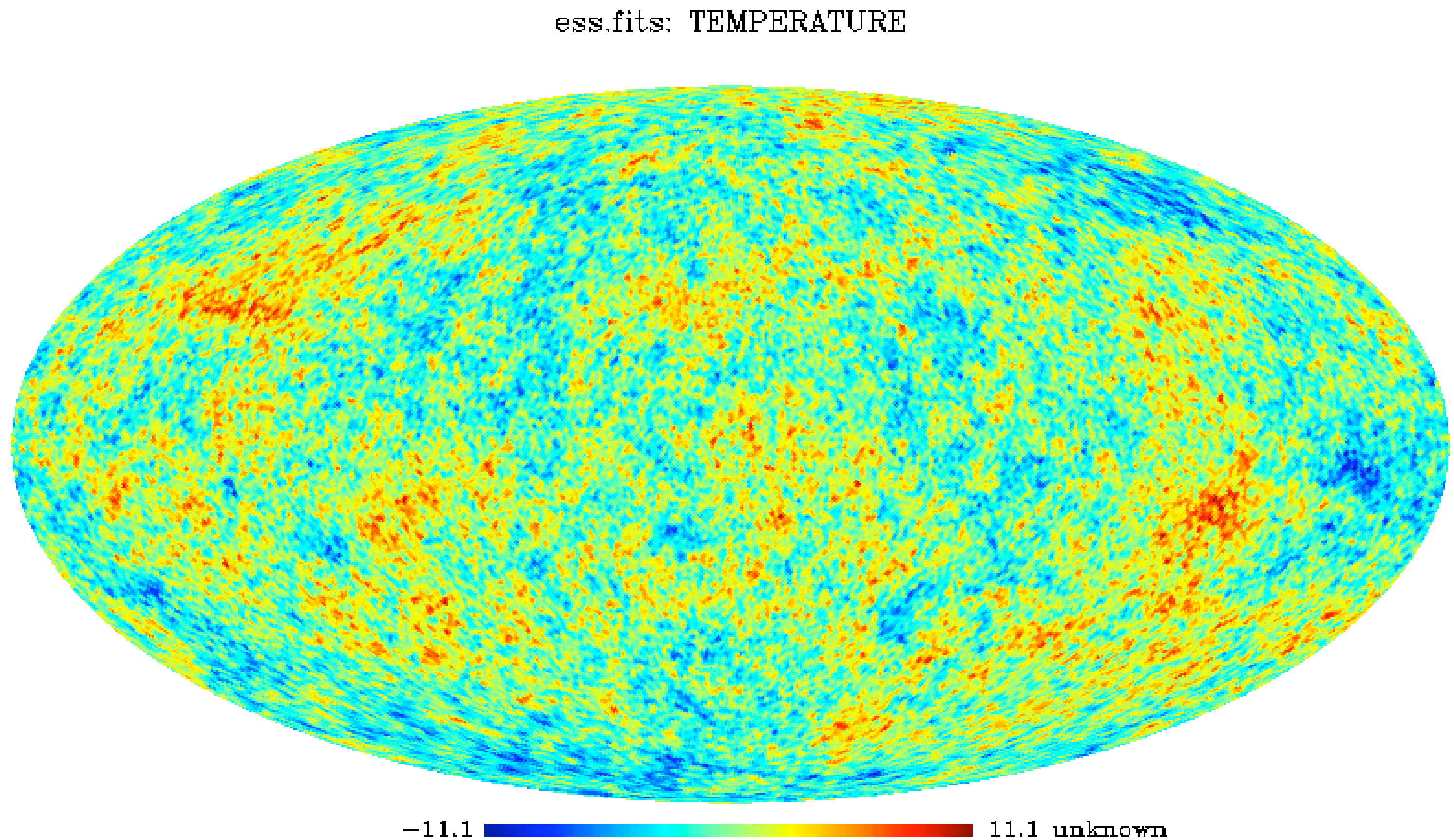
ess.fits: TEMPERATURE
−11.1
11.1 unknown

8result_h.fits: TEMPERATURE

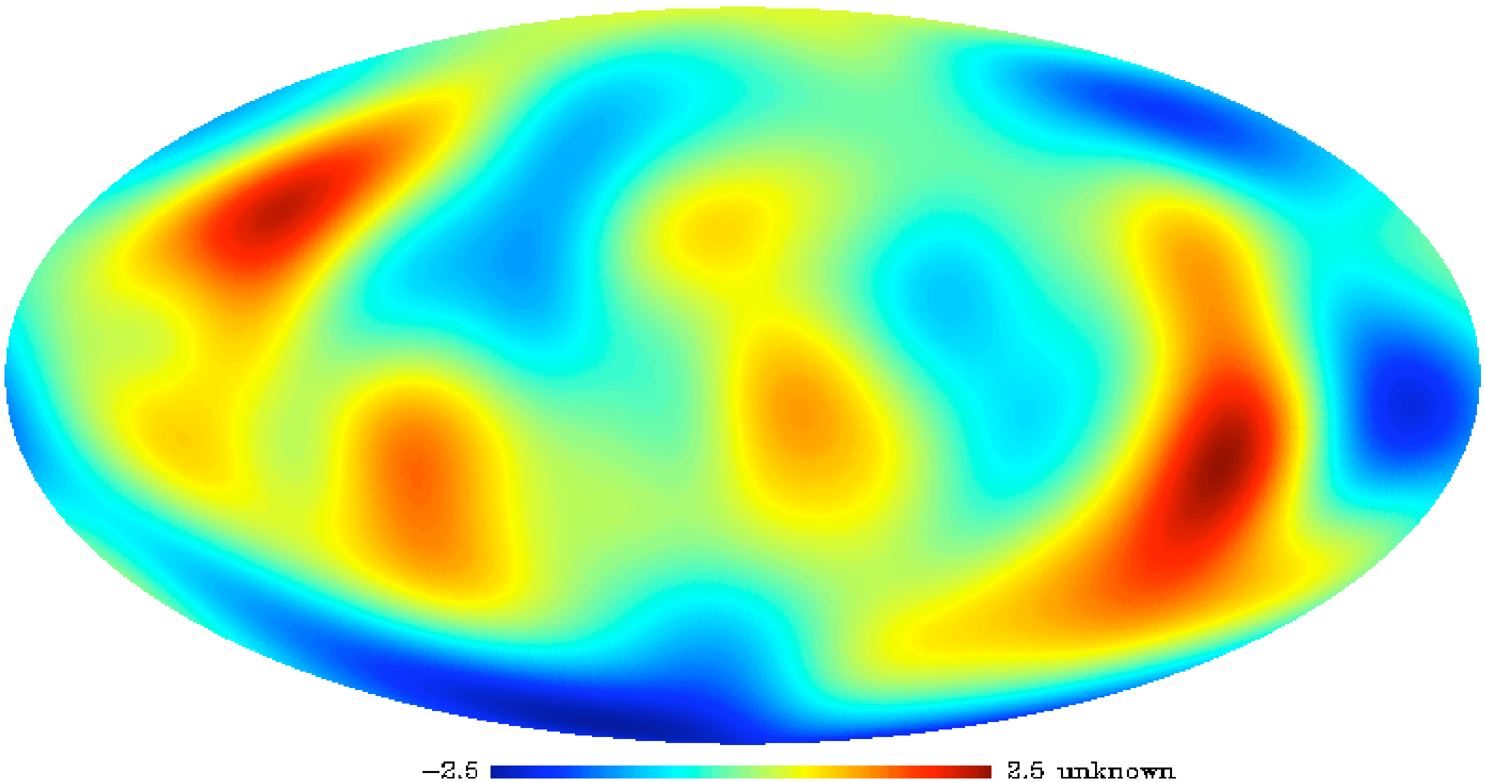

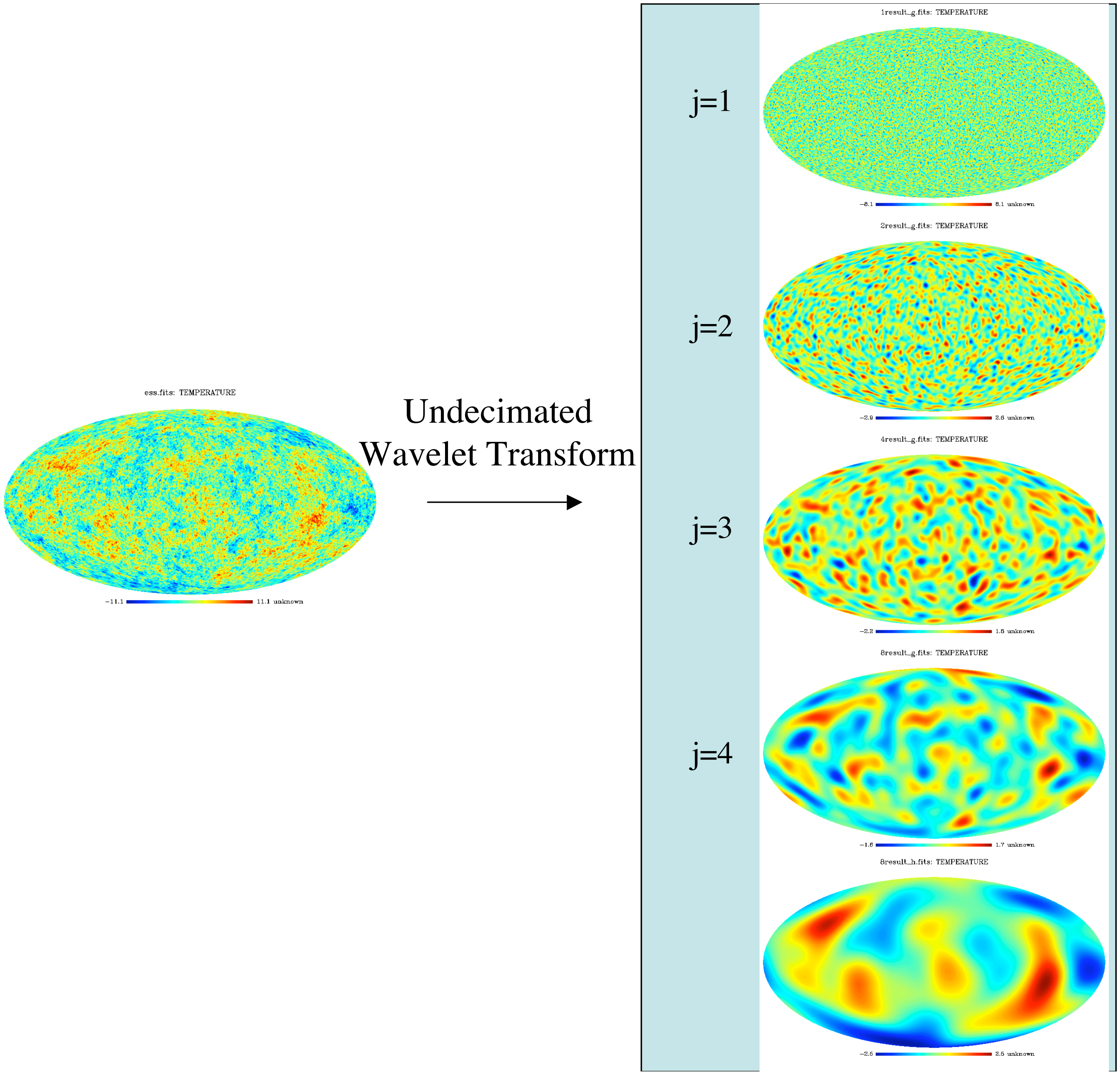
ess.fits: TEMPERATURE
−11.1
11.1 unknown
Undecimated
Wavelet Transform
j=1
1result_g.fits: TEMPERATURE
−8.1
8.1 unknown
j=2
2result_g.fits: TEMPERATURE
−2.9
2.6 unknown
j=3
4result_g.fits: TEMPERATURE
−2.2
1.8 unknown
j=4
8result_g.fits: TEMPERATURE
−1.6
1.7 unknown
8result_h.fits: TEMPERATURE
−2.5
2.5 unknown

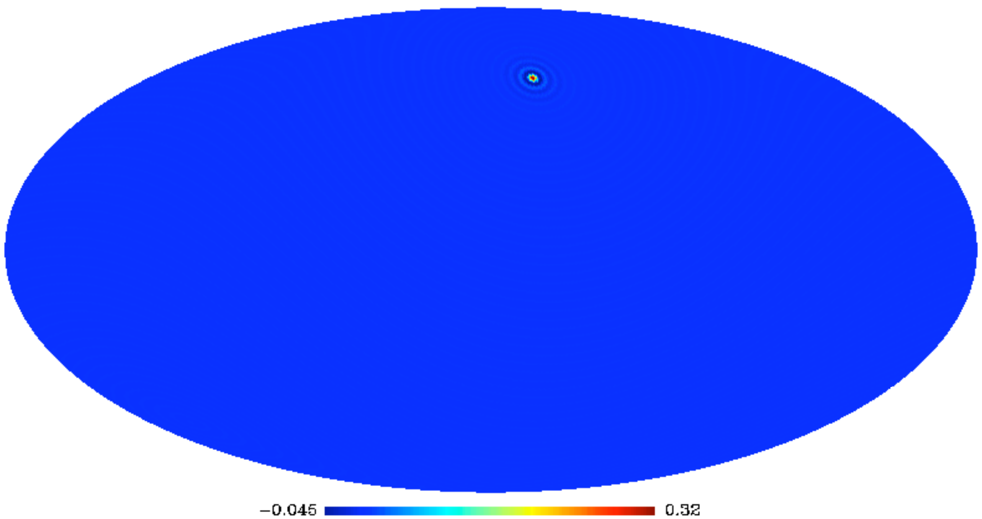

sky_recons.fits: X0

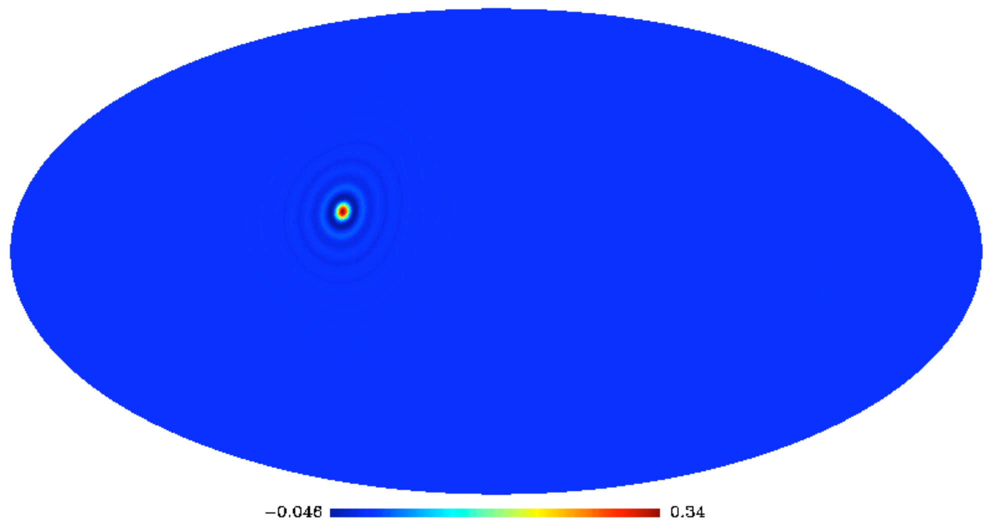

sky_recons.fits: X0

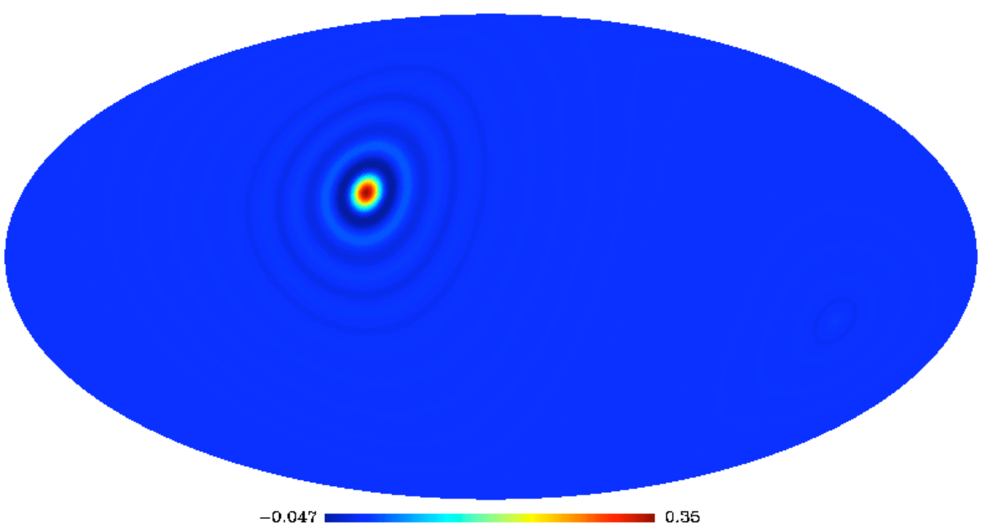

Pyramidal Wavelet Transform On the Sphere

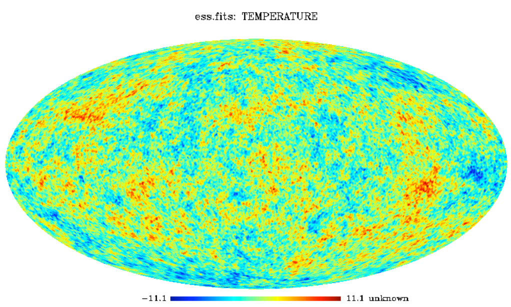

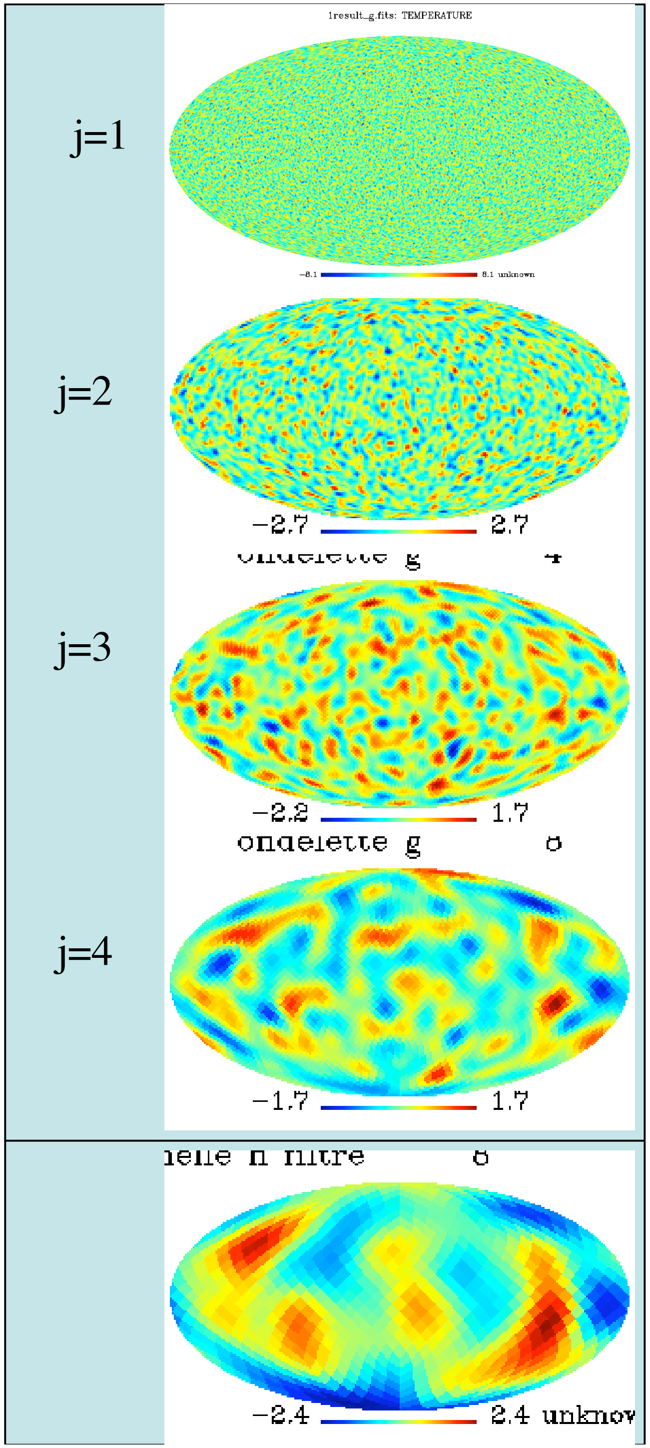

Ridgelets on the Sphere

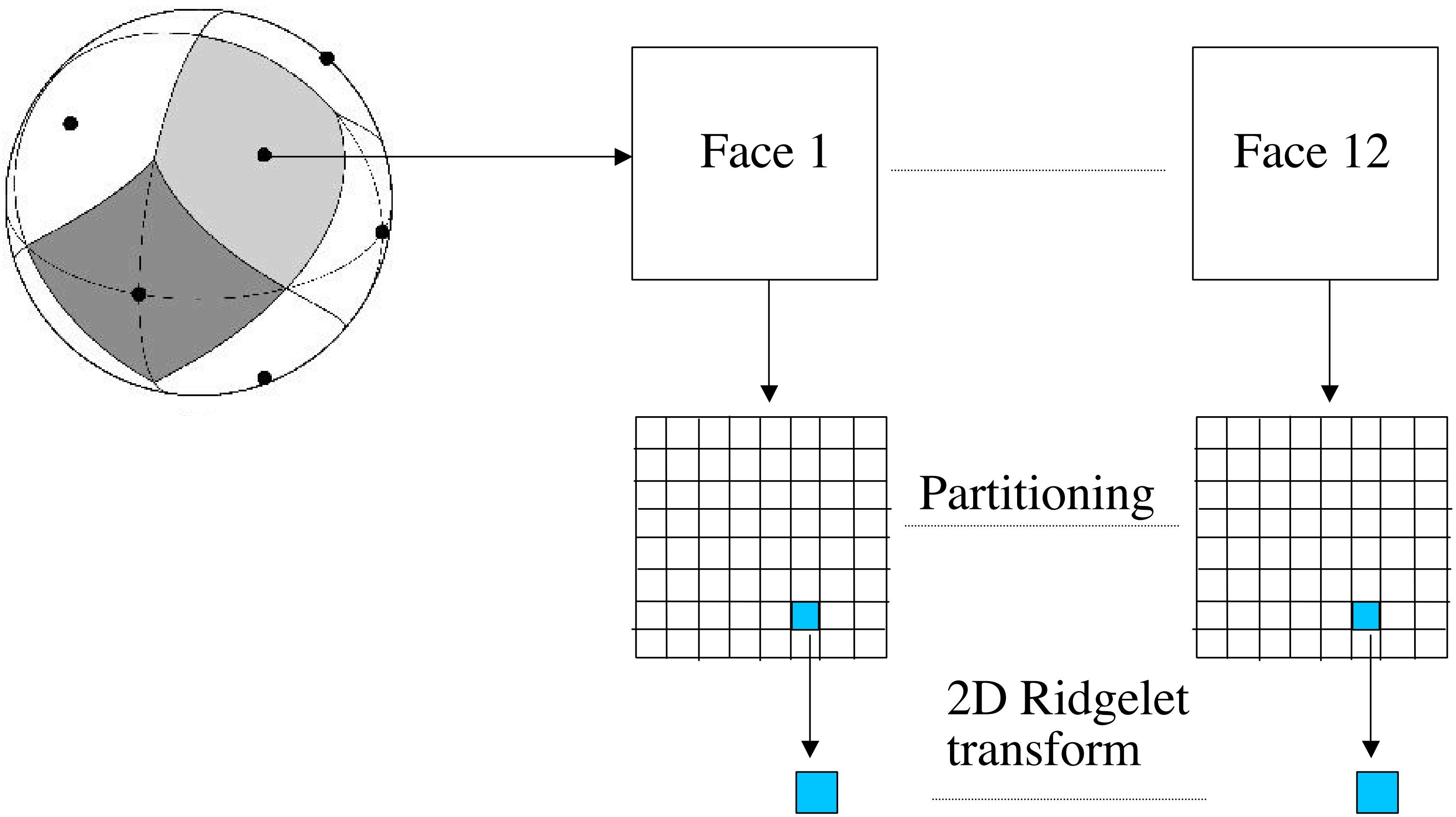

Example of ridgelet functions on the sphere

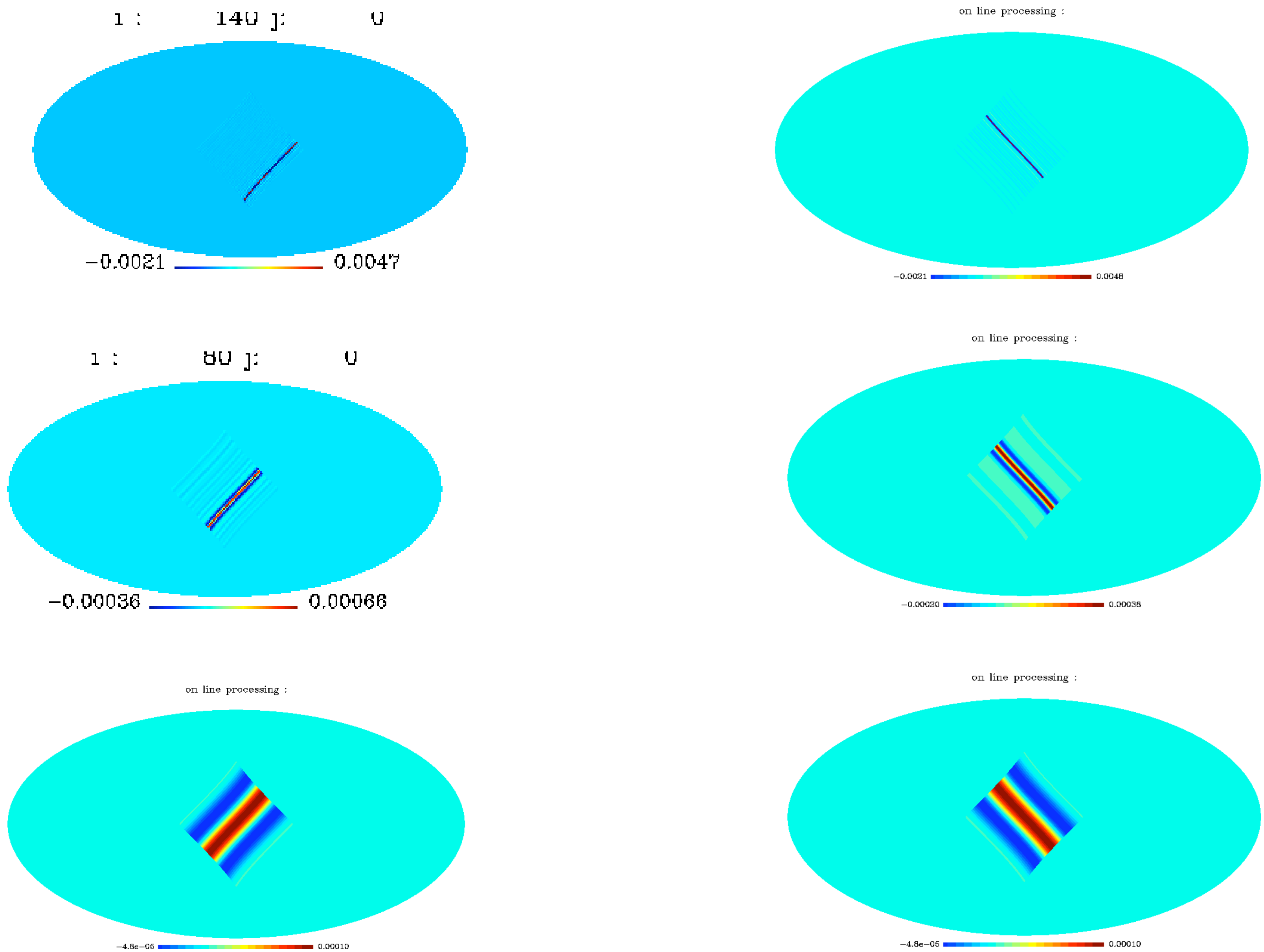

Curvelets on the Sphere

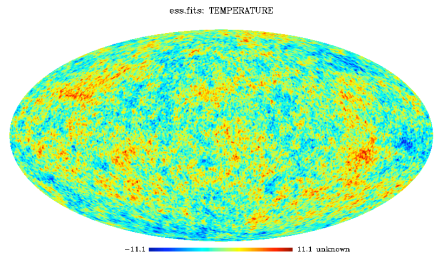

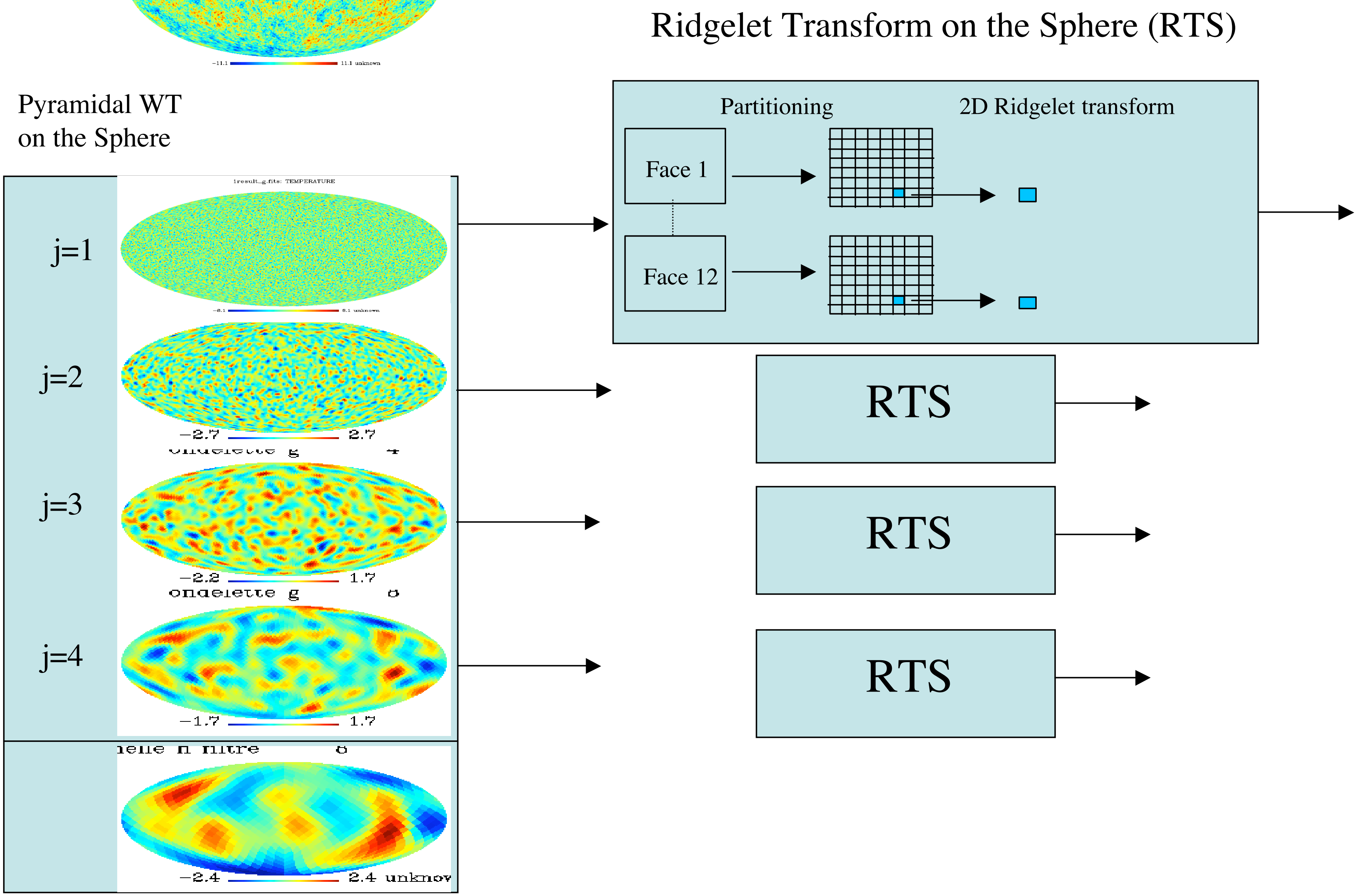

Example of curvelet functions on the sphere

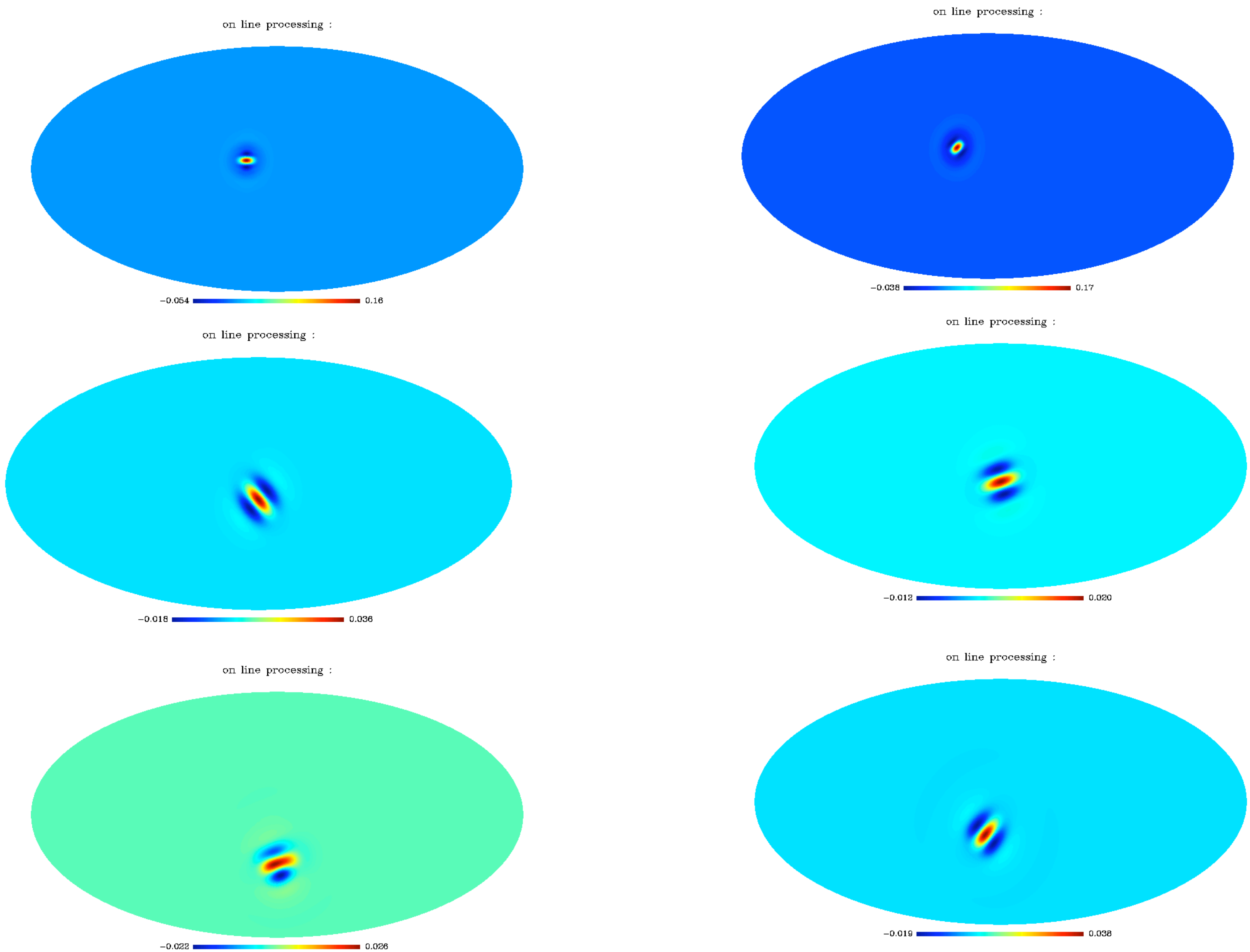

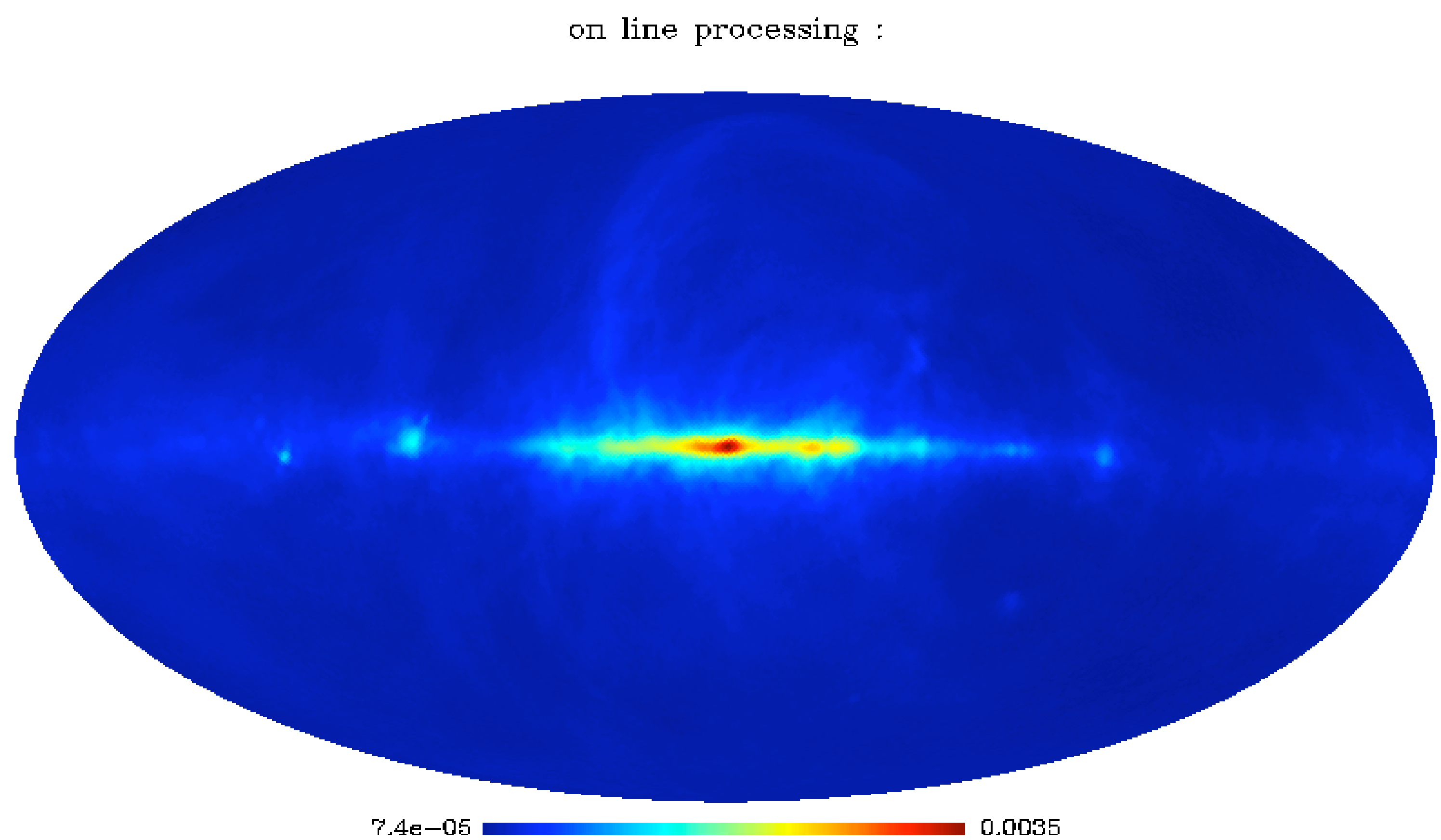
on line processing :
7.4e−05
0.0035

bruit1

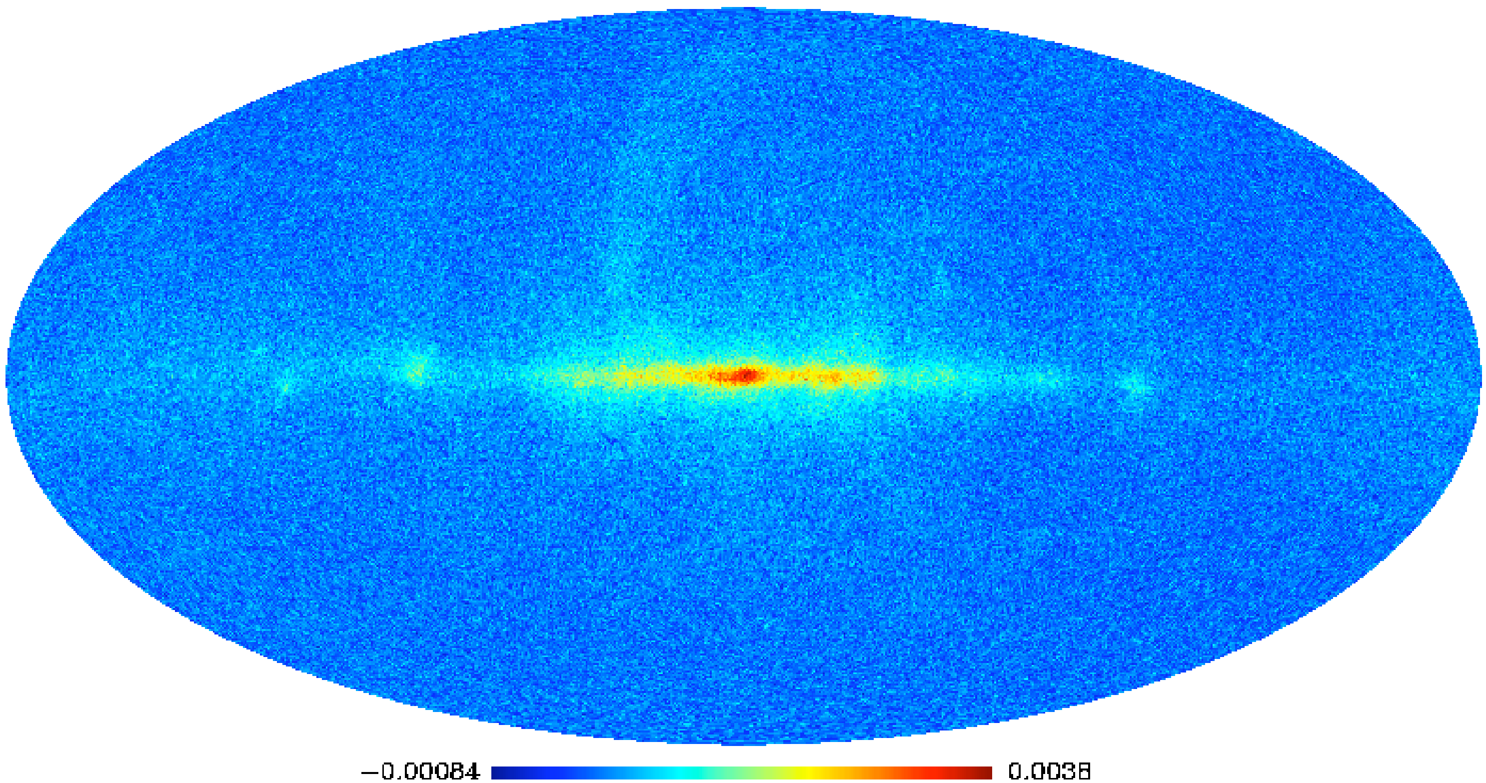

denoising cur at 5 sigma

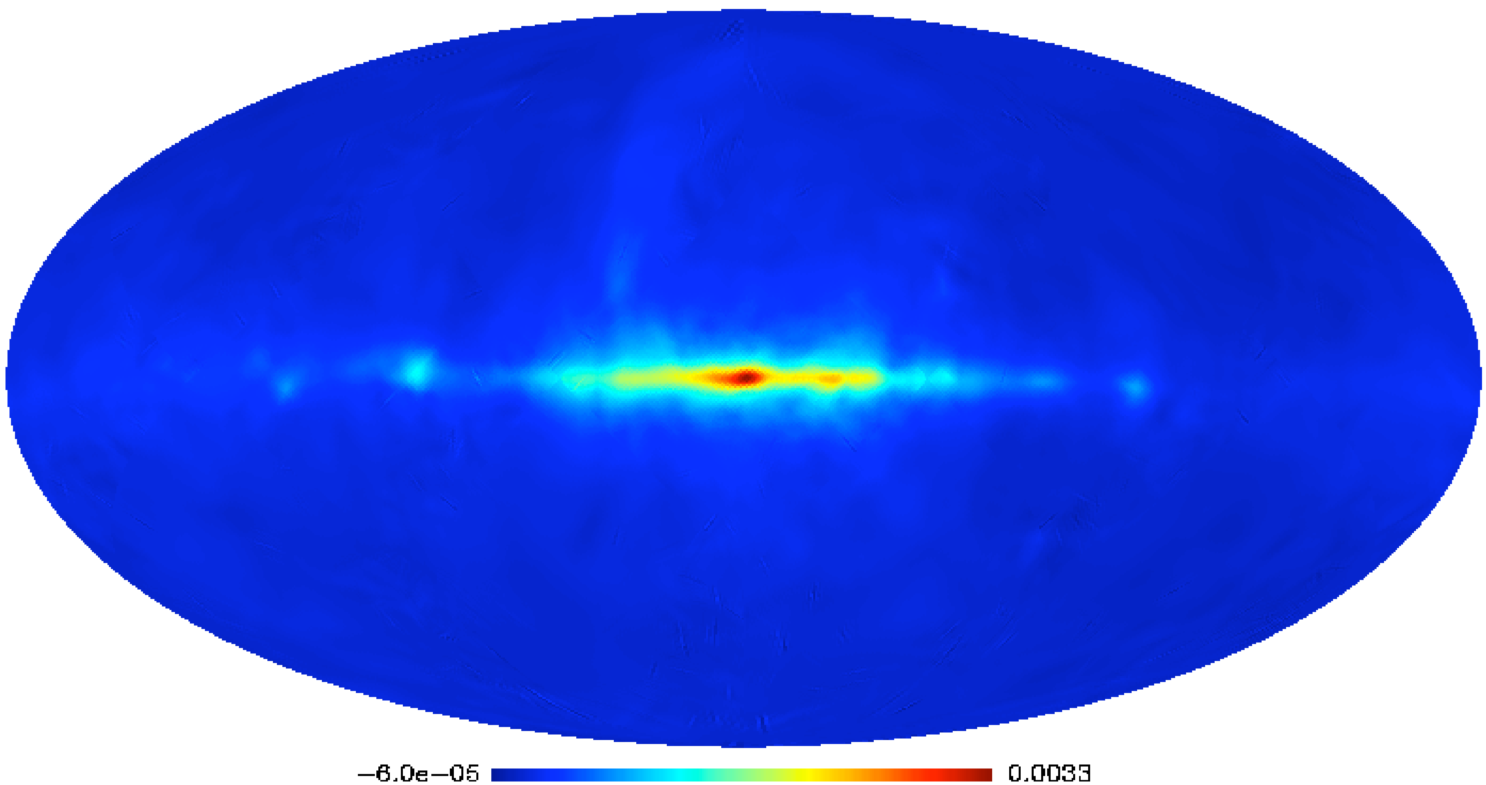

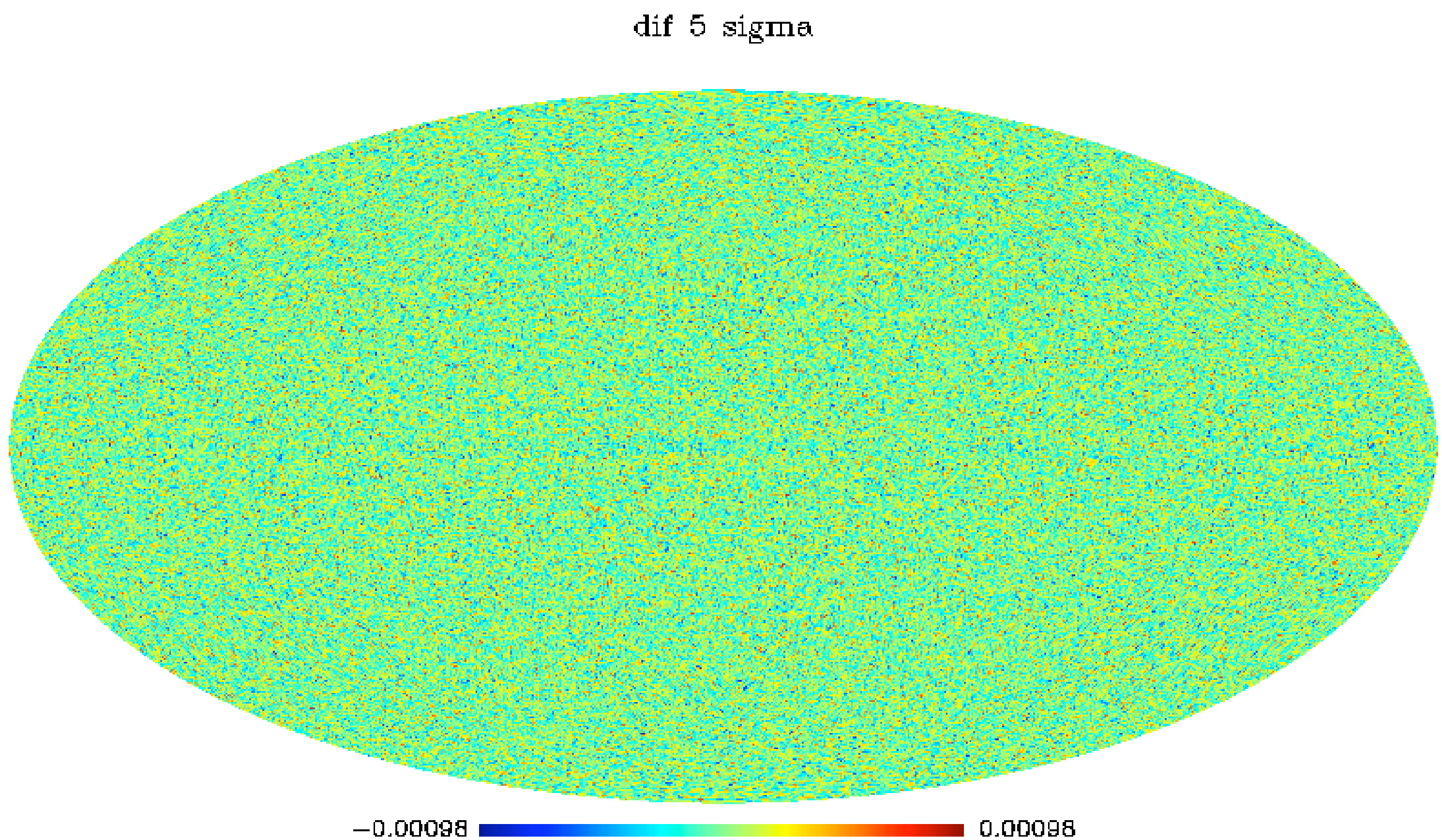
dif 5 sigma
−0.00098
0.00098

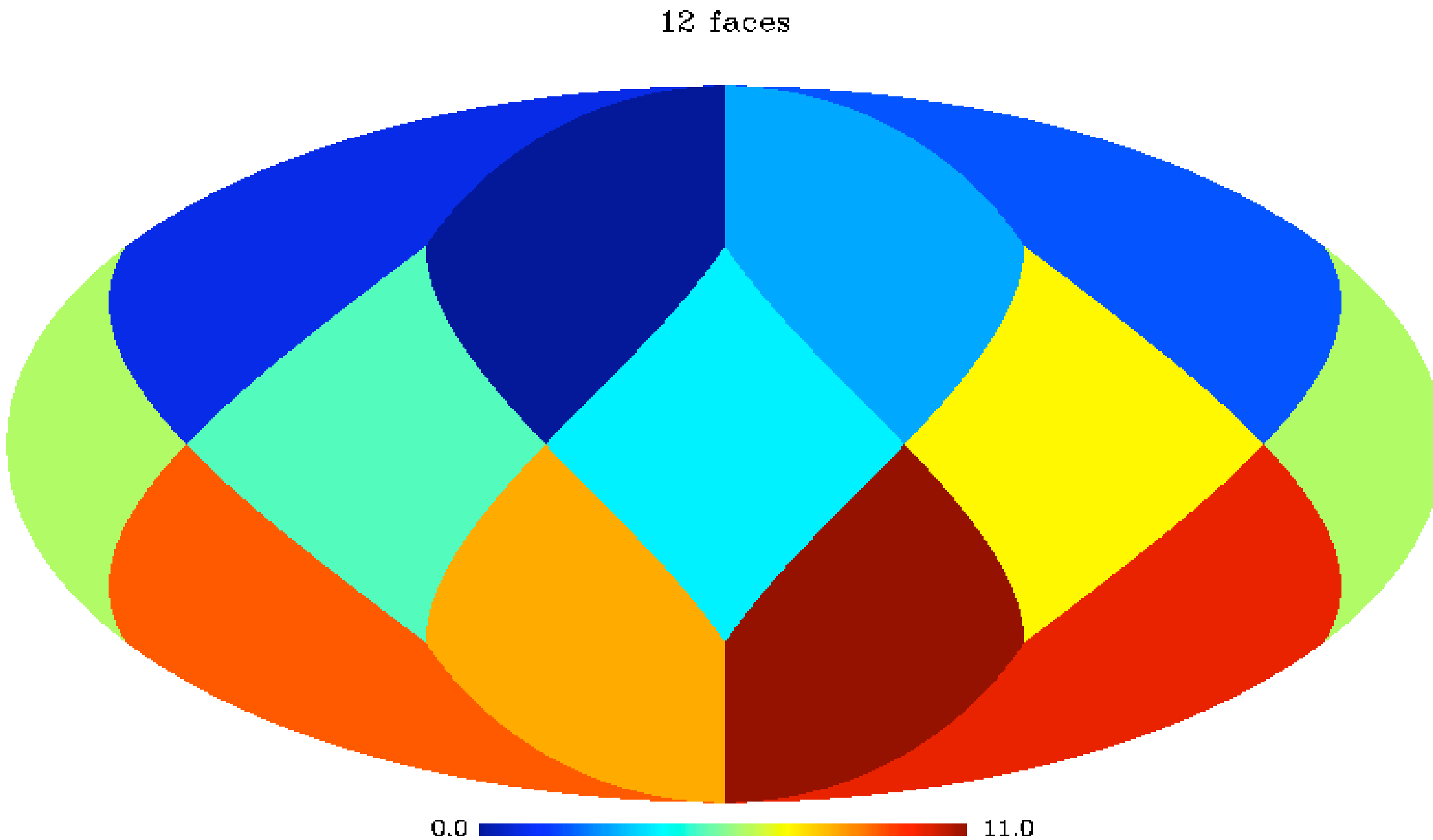
12 faces
0.0
11.0

12 faces rotation

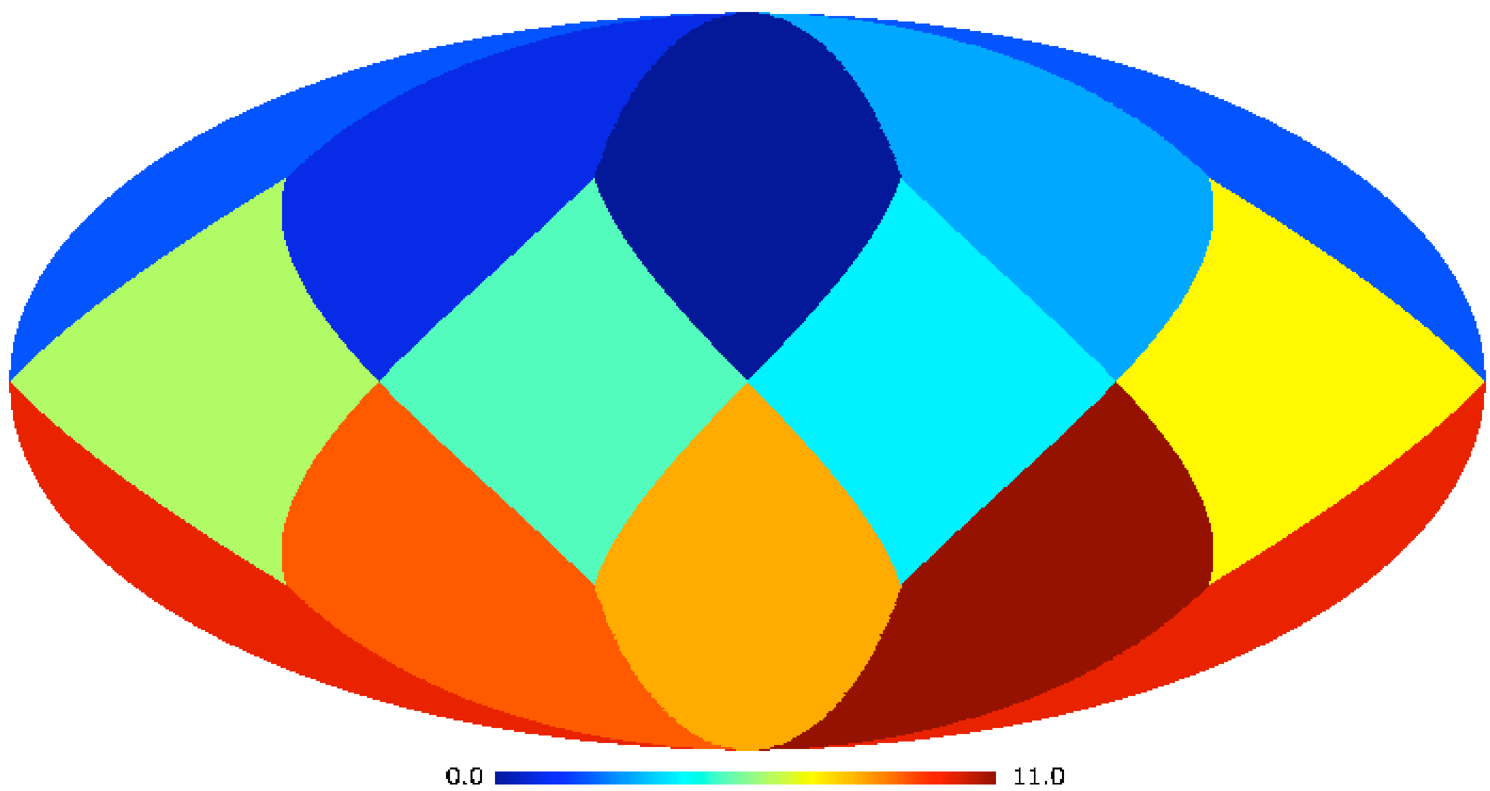

ponderation

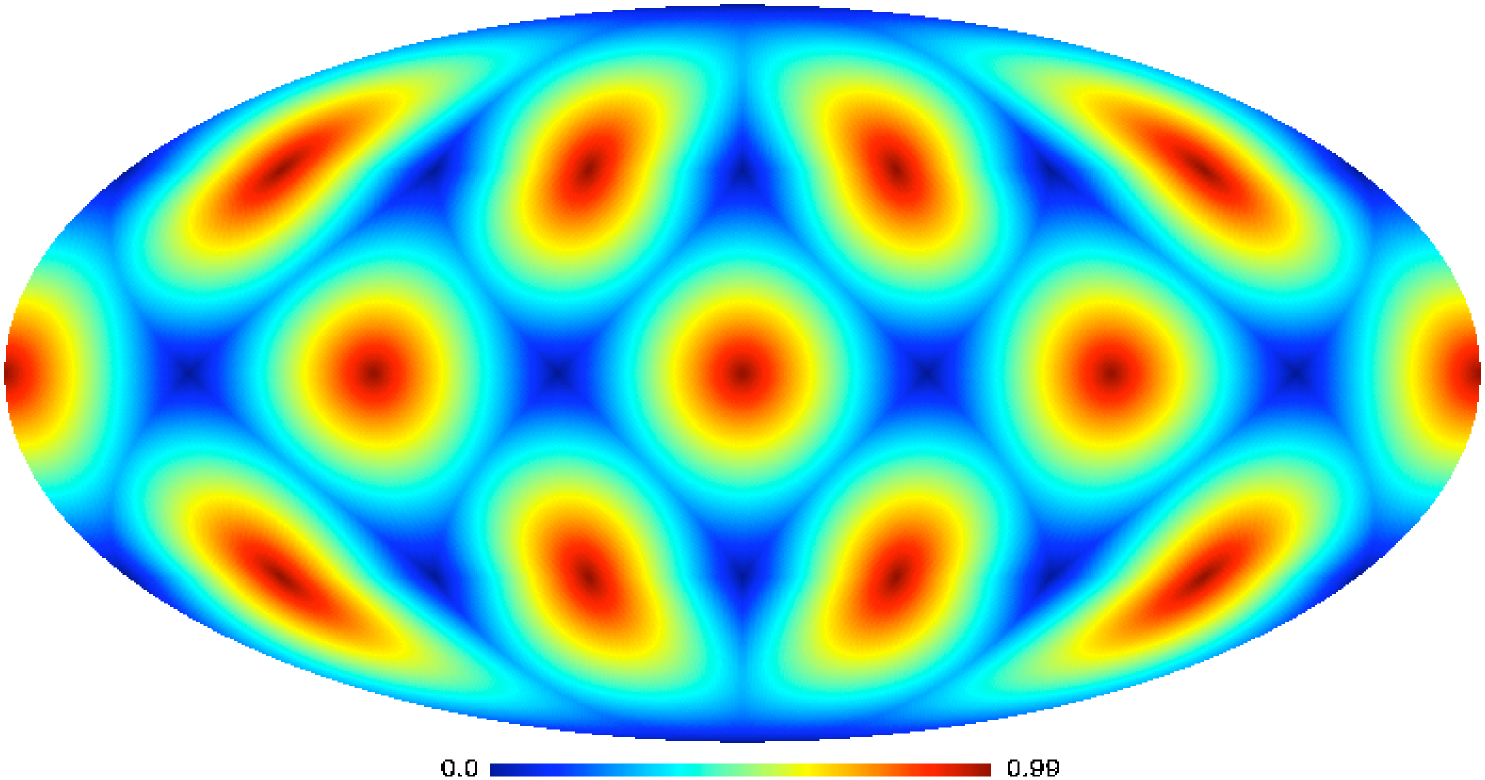

Conclusions

1. **Isotropic WT on the Sphere, very similar to the Isotropic a trous WT**

2. **Extension of CUR01 to the sphere**

3. **Produce encouraging results in our denoising experiment.**